Cellular and Molecular Life Sciences (2022) 79:213
https://doi.org/10.1007/s00018-022-04211-7

Cellular and Molecular Life Sciences

ORIGINAL ARTICLE

ER-mitochondria communication is involved in NLRP3 inflammasome activation under stress conditions in the innate immune system

Ana Catarina Pereira[1,2,3] · Jessica De Pascale[1] · Rosa Resende[1,3] · Susana Cardoso[1,3] · Isabel Ferreira[1,3,4] · Bruno Miguel Neves[5] · Mylène A. Carrascal[3,6] · Mónica Zuzarte[2,3,7] · Nuno Madeira[2,3,8,9] · Sofia Morais[2,3,9] · António Macedo[2,3,9] · Anália do Carmo[3,10] · Paula I. Moreira[1,2,3] · Maria Teresa Cruz[1,3,4] · Cláudia F. Pereira[1,2,3,11]

Received: 8 July 2021 / Revised: 14 February 2022 / Accepted: 16 February 2022 / Published online: 28 March 2022

Abstract

Endoplasmic reticulum (ER) stress and mitochondrial dysfunction, which are key events in the initiation and/or progression of several diseases, are correlated with alterations at ER-mitochondria contact sites, the so-called "Mitochondria-Associated Membranes" (MAMs). These intracellular structures are also implicated in NLRP3 inflammasome activation which is an important driver of sterile inflammation, however, the underlying molecular basis remains unclear. This work aimed to investigate the role of ER-mitochondria communication during ER stress-induced NLRP3 inflammasome activation in both peripheral and central innate immune systems, by using THP-1 human monocytes and BV2 microglia cells, respectively, as in vitro models. Markers of ER stress, mitochondrial dynamics and mass, as well as NLRP3 inflammasome activation were evaluated by Western Blot, IL-1β secretion was measured by ELISA, and ER-mitochondria contacts were quantified by transmission electron microscopy. Mitochondrial Ca^{2+} uptake and polarization were analyzed with fluorescent probes, and measurement of aconitase and SOD2 activities monitored mitochondrial ROS accumulation. ER stress was demonstrated to activate the NLRP3 inflammasome in both peripheral and central immune cells. Studies in monocytes indicate that ER stress-induced NLRP3 inflammasome activation occurs by a Ca^{2+}-dependent and ROS-independent mechanism, which is coupled with upregulation of MAMs-resident chaperones, closer ER-mitochondria contacts, as well as mitochondrial depolarization and impaired dynamics. Moreover, enhanced ER stress-induced NLRP3 inflammasome activation in the immune system was found associated with pathological conditions since it was observed in monocytes derived from bipolar disorder (BD) patients, supporting a pro-inflammatory status in BD. In conclusion, by demonstrating that ER-mitochondria communication plays a key role in the response of the innate immune cells to ER stress, this work contributes to elucidate the molecular mechanisms underlying NLRP3 inflammasome activation under stress conditions, and to disclose novel potential therapeutic targets for diseases associated with sterile inflammation.

Keywords Endoplasmic reticulum (ER) stress · Mitochondria · Unfolded protein response · Calcium · Sterile inflammation · Bipolar disorder (BD)

✉ Cláudia F. Pereira
cpereira@cnc.uc.pt; cpereira@fmed.uc.pt;
claudia.mf.pereira@gmail.com

1 CNC-Center for Neuroscience and Cell Biology, CIBB-Center for Innovative Biomedicine and Biotechnology, University Coimbra, Coimbra, Portugal

2 Faculty of Medicine, University Coimbra, Coimbra, Portugal

3 CACC-Clinical Academic Center of Coimbra, Coimbra, Portugal

4 Faculty of Pharmacy, University Coimbra, Coimbra, Portugal

5 iBiMED-Department of Medical Sciences and Institute for Biomedicine, University Aveiro, Aveiro, Portugal

6 Tecnimede Group, Sintra, Portugal

7 iCBR-Institute for Clinical and Biomedical Research, University Coimbra, Coimbra, Portugal

8 CIBIT-Coimbra Institute for Biomedical Imaging and Translational Research, University Coimbra, Coimbra, Portugal

9 Department of Psychiatry, CHUC-UC-Centro Hospitalar e Universitário de Coimbra, Coimbra, Portugal

10 Department of Clinical Pathology, CHUC-UC-Centro Hospitalar e Universitário de Coimbra, Coimbra, Portugal

11 Coimbra, Portugal

Abbreviations

ATF6	Activating transcription factor 6
ASC	Apoptosis associated speck-like protein containing a C-terminal caspase-activation-and-recruitment (CARD) domain
BCA	Bicinchoninic acid
BD	Bipolar disorder
BFA	Brefeldin A
Ca^{2+}	Calcium
CNS	Central nervous system
CHUC	Coimbra University's Hospitals
ER	Endoplasmic reticulum
ECF	Enhanced chemifluorescence
ERAD	ER-associated degradation
FBS	Fetal bovine serum
IMM	Inner membrane of mitochondrion
IRE1α	Inositol-requiring enzyme 1 α
IP_3R	Inositol trisphosphate Receptor
IL-1β	Interleukin-1 beta
IL-18	Interleukin-18
LPS	Lipopolysaccharide
MAMs	Mitochondria-associated membranes
MCU	Mitochondrial Ca^{2+} uniporter protein
mtDNA	Mitochondrial DNA
mPTP	Mitochondrial permeability transition pore
Mfn2	Mitofusin 2
MEFs	Mouse embryonic fibroblasts
NCLX	Na^+/Ca^{2+} exchanger
NLRP3	NOD-like receptor family pyrin domain-containing 3
OMM	Outer mitochondrial membrane
PRR	Pattern-recognition receptor
PBMCs	Peripheral blood mononuclear cells
PBS	Phosphate buffered saline
PVDF	Polyvinylidene difluoride
pro-IL-1β	Pro-interleukin-1 beta
PERK	Protein kinase R-like endoplasmic reticulum kinase
ROS	Reactive oxygen species
Rhod-2 AM	Rhodamine-2 acetoxymethyl ester
RT	Room temperature
SEM	Standard error of the mean
Sigma-1R	Sigma-1 receptor
SDS-PAGE	Sodium dodecyl sulphate–polyacrylamide gels
SOD	Superoxide dismutase
TEM	Transmission electron microscopy
TMRE	Tetramethyl-rhodamine ethyl ester
TLR	Toll-like receptor
TBS	Tris-buffered saline
TM	Tunicamycin
UPR	Unfolded protein response
VDAC	Voltage-dependent anion channel
Xest C	Xestospongin C
WB	Western Blot

Introduction

The endoplasmic reticulum (ER) is a multifunctional organelle involved in a wide variety of key cellular events, namely the synthesis, folding and maturation of secreted and transmembrane proteins. In addition to its role in proteostasis, ER also ensures the synthesis of phospholipids and steroids, and the storage of Ca^{2+} ions [1, 2]. The aberrant accumulation of unfolded and/or misfolded proteins in the lumen of this organelle induces ER stress.

Under ER stress conditions, an extremely conserved signaling cascade termed the unfolded protein response (UPR), which involves three specialized ER stress-sensing proteins namely protein kinase R-like endoplasmic reticulum kinase (PERK), inositol-requiring enzyme 1α (IRE1α) and the activating transcription factor 6 (ATF6), is induced to rescue cells from stress and restore ER homeostasis [3]. Once activated, the UPR triggers a set of transcriptional and translational events that decrease de novo protein synthesis, activate an antioxidant response, and increase the expression of genes encoding mediators of ER-associated degradation (ERAD) and autophagy, as well as ER-resident chaperones such as GRP78 [4, 5]. However, cell fate under stress conditions is determined by the extent and duration of ER stress [6]. Cells are able to cope with acute/mild-moderate ER stress and reestablish homeostasis by inducing pro-survival signaling pathways. Conversely, under chronic/severe ER stress, this adaptive response fails and a terminal UPR program commits cells to apoptosis [7]. Under irremediable ER stress, an inflammatory response can be also triggered involving the activation of the NLRP3 inflammasome [8].

The peculiar ER architecture, a cisternae-like structure extending from the nuclear envelope to the cell membrane, allows the establishment of inter-organelle communication networks that play a key role in preserving cell homeostasis. Accordingly, ER has been pointed out as a sensor for cell stress, since its connection with other organelles is promoted under stressful conditions to trigger a fast and effective response [9]. This can be illustrated by the stress-induced contact between ER and mitochondria, which promotes inter-organelle Ca^{2+} transfer thus preserving cell metabolism and ATP production [10]. In close contacts between these organelles, Ca^{2+} is released from ER-localized inositol trisphosphate receptor (IP_3R) and transferred to mitochondria through the voltage-dependent anion channel (VDAC) in the outer mitochondrial membrane (OMM), subsequently entering into the mitochondrial matrix by the mitochondrial Ca^{2+} uniporter protein (MCU), which is located in the inner membrane of the mitochondrion (IMM) [11].

The tight association between ER and mitochondria originates dynamic platforms, the so-called mitochondria-associated membranes (MAMs), which allow the physical and biochemical communication between the two organelles, ensuring an efficient inter-organelle exchange of Ca^{2+} ions and lipids, thus controlling mitochondrial bioenergetics and pro-survival/pro-death pathways [12–15]. Therefore, a proper distance between these organelles, which can range between 10 and 80–100 nanometers (nm), is crucial to the normal ER-mitochondria crosstalk. Alterations in proper distance between these organelles, by excess or lack of ER-mitochondria communication at MAMs, have been intimately associated with pathological conditions [16].

Although the molecular identity of MAM's resident proteins is still incomplete, it is known that ER-mitochondria juxtaposition is mediated by tethering proteins namely Mitofusin 2 (Mfn2), which can bind these organelles based on its strategic location on both OMM and the ER surface [1]. MAM's composition and abundance are highly dynamic being modulated by metabolic demands and cellular insults to promote cell adaptation according to cellular needs. These lipid raft-like ER subdomains also regulate mitochondrial dynamics, proteostasis, redox status, as well as inflammasome signaling [12–15].

Inflammasomes are cytosolic multiprotein complexes activated to initiate and sustain innate immune responses to harmful stimuli [17, 18]. They are typically constituted by a cytosolic pattern-recognition receptor (PRR), caspase-1, and the adaptor protein apoptosis-associated speck-like protein containing a C-terminal caspase-activation-and-recruitment (CARD) domain (ASC). When assembled, inflammasome activation is induced by the autocatalytic cleavage of caspase-1, which in turn leads to the release of mature interleukin-1 beta (IL-1β) and interleukin-18 (IL-18). These two pro-inflammatory cytokines have been strongly implicated in neuroimmunomodulation, neuroinflammation, and neurodegeneration [17–20]. Nowadays, NOD-like receptor family pyrin domain-containing 3 (NLRP3) inflammasome is the most relevant and studied inflammasome because its PRR, the NLRP3, responds to multiple activators [18, 20, 21].

The canonical inflammasome activation pathway is a two-signal model [17–20]. The first signal (priming step), triggered by toll-like receptor (TLR) ligands or endogenous molecules, upregulates the NLRP3 inflammasome-related components [22–24]. The second signal (activation step) induces the assembly of the above components and is provided by diverse stimuli such as ATP, pore-forming toxins, or particulate matter, among others [20]. Indeed, the fact that NLRP3 inflammasome may be activated by different stimuli suggests that it works as a general sensor of cellular damage and/or stress. Nowadays, the K^+ efflux is pointed out as the most consensual trigger for NLRP3 inflammasome activation [18, 20]. However, other physiological events including mitochondrial dysfunction and subsequent generation of mitochondrial reactive oxygen species (mtROS), release of mitochondrial DNA (mtDNA) or cardiolipin, the release of cathepsins into the cytosol after lysosomal destabilization, and ionic flux such as Ca^{2+} mobilization have also been pointed out as NLRP3 activating stimuli. Given that these events are not always implicated in NLRP3 inflammasome activation, the underlying mechanisms are still not fully understood, and more fine-tuned studies are required to decipher the molecular basis of NLRP3 inflammasome activation under specific stressful conditions [25].

In recent years, the relevance of MAMs in innate immunity has been risen, with MAMs being currently recognized as a signaling hub that regulates NLRP3 inflammasome-mediated inflammation [13, 15]. The main evidence of the close association between MAMs and NLRP3 inflammasome in immune cells is the subcellular localization of NLRP3 inflammasome-related components under pro-inflammatory conditions. In its inactive state, NLRP3 is localized in the ER membrane and cytosol, however, in the presence of NLRP3 inflammasome activators, both NLRP3 and ASC are translocated to MAMs platform [26]. Since major NLRP3 activators are mitochondria-derived molecular signals such as mtDNA and mtROS, it is hypothesized that the NLRP3 inflammasome is translocated to MAMs to sense damaging signals released from or residing in mitochondria [27]. In addition to mitochondria, ER also plays a key role in NLRP3 inflammasome activation. For instance, excessive ER Ca^{2+} release leads to mitochondrial Ca^{2+} overload, triggering NLRP3 inflammasome activation. The UPR pathway has also been implicated in NLRP3 activation, with IRE1α and PERK inducing the expression of IL-1β and NLRP3 via NF-κB pathway [28]. Recently, De la Roche and colleagues found that the trafficking of cholesterol to the ER is required for activation of the NLRP3 inflammasome [29].

Taken together, the ER-mitochondria proximity at MAMs platforms allows the physical interaction between the NLRP3 inflammasome and its ligands released from or residing in mitochondria, as well as the detection of signals that originated due to the failure of the ER adaptive capacity under chronic/severe ER stress [28]. The emerging role of MAMs as a modulator of innate immunity is further supported by evidence implicating abnormalities on ER-mitochondria axis in the onset and progression of several human pathological conditions strongly associated with inflammation, including cancer, diabetes, obesity, neurodegenerative and psychiatric disorders [1, 13, 30–32].

This study was aimed to investigate the effect of ER stress in peripheral and central innate immune system focusing on NLRP3 inflammasome activation, as well as to evaluate ER-mitochondria contact sites as the link between these events. Furthermore, we intend to disclose whether the ER stress-NLRP3 inflammasome axis is involved in a pathological

context, specifically on bipolar disorder (BD), a psychiatric illness that often leads to functional impairment and reduced quality of life, a burden that extends to family members [33].

Materials and methods

Materials

The THP-1 human monocytic cell line (ATCC TIB-202) was bought to InvivoGen, (Toulouse, France). The murine BV2 microglia cell line was bought to Biological and Cell Banking Factory, Centro di Risorse Biologiche (Genova, Italy). RPMI 1640 medium, penicillin, streptomycin, tunicamycin, brefeldin A, thapsigargin, bicinchoninic acid (BCA) protein assay kit, superoxide dismutase (SOD) activity kit, N-acetylcysteine (NAC), Xestospongin C (Xest C) and tetramethyl-rhodamine ethyl ester (TMRE) probe were obtained from Sigma Chemical Co. (St. Louis, MO, USA). The fluorescence probes Hoechst 33342 and Rhodamine-2 acetoxymethyl ester (Rhod-2 AM) were obtained from Invitrogen (Eugene, OR, USA). Ru360 and potassium cyanide (KCN) were obtained from Merck (Kenilworth, NJ, USA). Fetal bovine serum (FBS) and all reagents for primary monocytes culture including RPMI 1640 medium HEPES no glutamine, penicillin, streptomycin, sodium pyruvate, glutamax, non-essential amino acids and heat-inactivated fetal bovine serum (FBS) were obtained from Gibco, Thermo Fisher Scientific (Waltham, MA, USA). The human monocytes isolation kit II was obtained from Miltenyi Biotec (Bergisch, Gladbach, Germany). Both legend MAX Human IL-1β ELISA kit with precoated plates and MAX Deluxe set Human IL-1β without precoated plates were obtained from Biolegend (San Diego, CA, USA). The protease and phosphatase inhibitor cocktails were obtained from Roche (Mannheim, Germany), and NZY colour protein marker II was from NZYTech (Lisbon, Portugal). The ficoll-paque plus, alkaline phosphatase-linked secondary antibodies and the enhanced chemifluorescence (ECF) reagent were obtained from GE Healthcare (Chalfont St. Giles, UK), and the polyvinylidene difluoride membranes were from Millipore Corporation (Bedford, MA, USA). Antibodies against phospho-eIF2α, eIF2α, ATF4, CHOP, IRE1α, Sigma-1R, phospho-DRP1, PDI, NLRP3 and ASC were from Cell Signaling Technology (Danvers, MA, USA). The anti-XBP1s and DRP1 antibodies were from Biolegend (San Diego, CA, USA). Anti-Mitofusin 2, IL-1β, ND1, TFAM, TOM20 and ERO1α antibodies were from Santa Cruz Biotechnology (Dallas, TX, USA), anti-GRP78 was from BD Biosciences (San Jose, CA, USA) and anti-MTCO1 was from Abcam (Cambridge, MA, USA). Epoxy resin was obtained from Fluka Analytical, (Germany). All other reagents were from Sigma Chemical Co. (St. Louis, MO, USA).

Methods

Cell lines culture

The THP-1 human monocytic cell line was cultured and maintained in 75 cm^2 flasks at a cell density between $0.5–1.0 \times 10^6$ cells/mL in RPMI 1640 medium supplemented with 10% (v/v) heat-inactivated fetal bovine serum (FBS), 25 mM glucose, 10 mM Hepes, 1 mM sodium pyruvate, 100 U/mL penicillin and 100 µg/mL streptomycin. Cells were maintained at 37 ºC in a humidified incubator under an atmosphere containing 5% CO_2. Cells were subcultured every 2–3 days and kept in culture for a maximum of 2 months.

The murine BV2 microglia cell line was cultured and maintained at a density of 1×10^5 cells/cm^2 in RPMI 1640 medium supplemented with 23.8 mM sodium bicarbonate10% (v/v) heat-inactivated FBS, 100 U/mL penicillin and 100 µg/mL streptomycin. Cells were maintained at 37 ºC in a humidified incubator under an atmosphere containing 5% CO_2.

Isolation and culture of primary human monocytes

Participants of the disease group were selected among 18–35 years-old patients with BDI in early phases—BD stage 2 [34] followed at the Psychiatry Department from Coimbra University's Hospitals (CHUC), Coimbra, Portugal, and were assessed regarding a DSM-5 [35] BD diagnosis through a validated diagnostic interview [34, 36]. Matched unaffected controls were selected among students and health professionals from Coimbra University. Human peripheral blood was collected by vein puncture from male BD patients and healthy gender- and age-matched controls, upon written informed consent and approval of the study by the Ethical Committee from the same institution (150/CES, July 3rd). Hematological and biochemical parameters were analyzed in approximately 2–3 mL of collected blood at the CHUC's Clinical Pathology service and the remaining volume (~ 20 mL) was used for isolation of monocytes. Primary human monocytes were isolated and cultured as previously described [37].

Protein analysis by immunoblot

Total cell lysates for Western Blot (WB) analysis were prepared from THP-1 cells plated in 6-well plate at a density of 2.4×10^6 cells/well and treated with 5 or 10 µg/mL tunicamycin (TM) for the indicated time periods (1–24 h). Primary monocytes isolated from BD patients and controls were plated in 12-well plates at a density of 1.2×10^6 cells/well and then treated with TM 5 or 10 µg/mL for 8 h. BV2

cells were plated at a density of 1×10^5 cells/cm^2 and treated with brefeldin A (BFA, 2 or 10 µM) for 6 h.

After incubation with ER stressors, cells were washed with cold PBS, pH 7.4 and lysed on ice with an ice-cold lysis RIPA buffer [50 mM Tris–HCl (pH 8.0), 1% (v/v) Nonidet P-40, 150 mM NaCl, 0.5% (w/v) sodium deoxycholate, 0.1% (w/v) SDS, 2 mM EDTA, and 1 mM DTT] freshly supplemented with a protease and phosphatase inhibitor cocktail. Nuclei and insoluble cell debris were removed by centrifugation at 12000*g* for 10 min at 4 °C and the supernatant was collected and stored at −80 °C until further use. The total protein amount was quantified using the bicinchoninic acid (BCA) method. Then, proteins present in cell lysates were denatured in sample buffer [5% (w/v) SDS, 0.125 M Tris–HCl pH 6.8, 20% (v/v) glycerol, 10% (v/v) 2-mercaptoethanol and bromophenol blue] and heated for 5 min at 95 °C.

Briefly, proteins (40 µg in THP-1 and BV2 cell lines, or 30 µg in primary monocytes) were separated by electrophoresis on a 10% (v/v) sodium dodecyl sulphate–polyacrylamide gels (SDS-PAGE) at 130 V for 60–75 min and then transferred from the gel to a methanol-activated polyvinylidene difluoride (PVDF) membrane by electroblotting using a Trans-Blot Cell wet transfer system (Bio-Rad, USA), at 400 mA, during 3 h, at 4 °C. After blocking with 5% (w/v) nonfat dry milk in Tris-buffered saline [(TBS): 150 mM NaCl, 25 mM Tris–HCl pH 7.6] containing 0.1% (v/v) Tween 20 (TBS-T) for 1 h, at RT, membranes were further incubated with the primary antibodies prepared in TBS-T with 1% (w/v) milk, overnight, at 4 ºC. Afterwards, membranes were washed with TBS-T and incubated at RT, during 1 h, with alkaline phosphatase-conjugated secondary anti-rabbit (1:20,000), anti-mouse (1:20,000) or anti-goat (1:20,000) antibodies, depending on the source of each primary antibody. The immune complexes were detected with the enhanced chemifluorescence (ECF) reagent using the imaging system Typhoon FLA 9000 (GE Healthcare, UK), following a new washing step with TBS-T. Total Lab TL 120 software was used to quantify the optical density of the bands. Results obtained were normalized to β-tubulin I or actin, which were used as a protein loading control in the assays with THP-1 and BV2 cells, respectively. In the end, results were normalized to untreated cells (control condition).

Transmission electron microscopy (TEM)

Cells were plated in 6-well plates at a density of 2.4×10^6 cells/well and were then treated with 5 or 10 µg/mL TM for 8 h. After treatment, cells were collected and centrifuged at 1008 g, for 5 min. The supernatant was discarded and the pellets were fixed with 2.5% (w/v) glutaraldehyde in 0.1 M sodium cacodylate buffer (pH 7.2) for 2 h. Cells were rinsed in the same buffer and post-fixation was performed using 1% (w/v) osmium tetroxide for 1 h. After rinsing in buffer, buffer and distilled water and a final rinsing step in distilled water, 1% (w/v) aqueous uranyl acetate was added to the cells for 1 h, for contrast enhancement. After rising in water, cells pellets were embedded in 2% (w/v) molten agar, and dehydrated in ethanol (30–100%). Then, cells were impregnated and included in Epoxy resin. After polymerization, ultrathin sections were mounted on copper grids and observations were carried out on a FEI-Tecnai G^2 Spirit Bio Twin electron microscope at 100 kV (FEI, USA). Image J (Fiji) was the software used to measure the ER width, as well as the distance between ER and mitochondria in control and TM-treated cells. Results express the number of ER-mitochondria contacts (≤ 100 nm) and, in particular, the number of close ER-Mitochondria contacts (≤ 15 nm), both calculated relatively to mitochondria number.

Measurement of mitochondrial citrate synthase activity

To evaluate mitochondrial citrate synthase activity, THP-1 cells were plated in 6-well plate at a density of 2.4×10^6 cells/well and treated with 5 or 10 µg/mL TM for 8 h. Then, cells were washed with ice-cold PBS and then homogenized in extraction buffer (0.25 M sucrose and 5 mM HEPES, pH 7.4) and protein content was quantified using the BCA method. In a 96 well-plate, 40 µg of the sample were added to 200 mM Tris–HCl (pH 8.0) reaction buffer containing 10% (v/v) Triton X-100, 10 mM DTNB, 10 mM acetyl-CoA, and the final volume per well was adjusted with water. Baseline was measured at 412 nm for 3 min at 30 °C. The reaction was started with 10 mM oxaloacetate and the reduction of DTNB was followed spectrophotometrically in a SpectraMax Plus 384 microplate reader (Molecular Devices LLC, California, USA) during 6 min. Results were expressed as nmol/min/mg protein.

Measurement of aconitase activity

To determine aconitase activity, THP-1 cells were plated in 6-well plate at a density of 2.4×10^6 cells/well and treated with 5 or 10 µg/mL TM for 8 h. Briefly, total cell extracts were washed with ice-cold PBS and then homogenize in ice-cold buffer (50 mM Tris–HCl, pH 7.4, and 0.6 mM $MnCl_2$ and 0.5% Triton-X 100), undergoing three cycles of freezing/thawing in liquid nitrogen and centrifuged at 10,000*g* for 10 min at 4 °C. After protein quantification by the BCA method, 40 µg of each sample were added to aconitase activity buffer (50 mM Tris–HCl and 0.6 mM $MnCl_2$, pH 7.4). The activity of cis-aconitase was monitored after the addition of 20 mM isocitrate for 20 min at 25 °C, by using

a SpectraMax Plus 384 microplate reader set to 240 nm (Molecular Devices LLC, California, USA). Results were expressed as U/mg protein/min.

Determination of superoxide dismutase (SOD) enzymatic activity

An enzymatic SOD assay was used to quantify SOD1 and SOD2 activities in response to ER stress, according to the manufacturer's instructions. For this purpose, THP-1 cells were plated in 6-well plate at a density of 2.4×10^6 cells/well and treated with 5 or 10 µg/mL TM for 4 h. Total cell lysates were obtained as previously described in the "Protein analysis by immunoblot" section, using RIPA buffer without supplements. Cell lysates were plated in a 96-well in duplicate and one well of each condition was incubated with 2 mM KCN to selectively inhibit SOD1 activity. The plate was then incubated at 37 °C for 20 min, and the absorbance was read in a spectrophotometer Synergy HT Multi Detection Microplate Reader (BioTek Instruments, Winooski, USA) set to 450 nm. SOD1 activity was determined by subtracting SOD2 activity from the total SOD activity. Values were normalized to the protein amount determined by the BCA method in each condition. Results were calculated relatively to untreated (control cells).

Determination of mitochondrial calcium uptake

Rhodamine-2 acetoxymethyl ester (Rhod-2/AM) fluorescent probe was used to evaluate Ca^{2+} influx into mitochondria in TM-treated and untreated THP-1 monocytes. For that purpose, cells were plated in 12-well plate at a density of 1.2×10^6 cells/well and treated with 5 or 10 µg/mL TM for 4 or 8 h.

After wash with a modified Krebs–Ringer buffer [Buffer A: 135 mM NaCl, 5 mM KCl, 1 mM $MgCl_2$, 20 mM HEPES, 1 mM $MgSO_4$, 0.4 mM KH_2PO_4; pH 7.4, complete before use by adding 1 mM $CaCl_2$ and 5.5 mM glucose], cells were incubated with 10 µM Rhod-2/AM prepared in buffer A for 45 min at 37 °C. Once washed with a Ca^{2+} -free modified Krebs–Ringer buffer [Buffer B: 135 mM NaCl, 5 mM KCl, 1 mM $MgCl_2$, 20 mM Hepes, 1 mM MgSO4, 0.4 mM KH_2PO_4, 0.5 mM EGTA; pH 7.4, supplemented with 5.5 mM glucose before use], cells were then resuspended in the same solution and the basal fluorescence values were monitored for 90 s, every 30 s. After a pulse of thapsigargin (1 µM), which induces ER Ca^{2+} depletion, fluorescence values were recorded for 700 s, every 10 s. SpectraMax Plus 384 microplate reader (Molecular Devices LLC, California, USA) was set to 552 nm excitation and 581 nm emission wavelengths. Results express the difference between the highest post-thapsigargin value and the mean of baseline levels, and were calculated relatively to control cells.

Determination of mitochondrial membrane potential

Tetramethylrhodamine ethyl ester (TMRE) fluorescence probe was used to evaluate alterations in mitochondrial membrane potential upon ER stress. THP-1 monocytes were plated in a 48-well plate at a density of 0.3×10^6 cells/well and treated with 5 or 10 µg/mL TM for 4 or 8 h. After incubation with 1 µM TMRE in PBS containing 0.2% (w/v) BSA for 30 min at 37 °C, cells were resuspended in PBS containing 0.2% (w/v) BSA and the fluorescence was monitored with a Synergy HT Multi Detection Microplate Reader (BioTek Instruments, Winooski, USA) set to 549 nm excitation and 575 nm emission wavelengths. Results were normalized to cells in the absence of TM exposure (control condition).

Measurement of secreted IL-1β levels

THP-1 cells were plated in 12-well plates at a density of 1.2×10^6 cells/well and then incubated with 5 or 10 µg/mL TM for 8 h upon priming with 1 µg/mL lipopolysaccharide (LPS) for 24 h, or only with LPS. As a positive control, THP-1 cells were exposed to 1 µg/mL LPS for 24 h plus 5 mM ATP for 30 min. When tested, the selective inhibitors of the IP_3R and of the MCU, Xestospongin C (Xest C, 1 µM) and Ru360 (10 µM), respectively, as well as the antioxidant N-acetylcysteine (NAC, 5 mM), were pre-incubated during 1 h. BV2 microglial cells were plated at a density of 1×10^5 cells/cm^2 and then treated with 2 or 10 µg/mL BFA during 6 h, upon priming with LPS (300 ng/ml) for 3 h. Primary monocytes isolated from BD patients and matched controls were plated in a 96-well plate at a density of 0.12×10^6 cells/well in a final volume of 0.15 mL and treated with TM (10 µg/mL) for 32 h.

To quantify the secretion of IL-1β induced by ER stress in THP-1 monocytes, BV2 microglial cells and primary human monocytes, an ELISA kit was used according to the manufacturer's instructions. Briefly, cells were centrifuged at 400 g for 5 min and the supernatants were collected and stored at −80 °C for subsequent use. Absorbance values were measured in a standard Synergy HT Multi Detection Microplate Reader (BioTek Instruments, Winooski, USA) set to 450 nm and 570 nm wavelengths. IL-1β secreted levels were expressed as pg/mL. In the case of THP-1 monocytes, results were calculated relatively to LPS-treated cells.

Evaluation of cell viability

Susceptibility towards ER stress was evaluated in THP-1 human monocytes by the resazurin assay. THP-1 cells were cultured in a 96-well plate at a density of 0.2×10^6 cells/well and treated with 5 or 10 µg/mL TM for the indicated time periods (4, 8 or 24 h). Cells were incubated with resazurin solution (50 µM) 4 h before the end of treatment, at 37 ºC. In the case of TM treatment for 4 h, the ER stressor and resazurin solution were added at the same time. Absorbance values were measured at 570 and 600 nm in a Synergy HT Multi Detection Microplate Reader (BioTek Instruments, Winooski, USA), and the final values were obtained from the subtraction of results determined at 600 nm from those measured at 570 nm. Cell viability was determined as the percentage (%) of controls, in the absence of TM.

Hematological and biochemical parameters from bipolar disorder patients and healthy controls

Blood samples collected in K_3EDTA tubes were evaluated on the Sysmex XN automated hematology analyzer (Sysmex, Kobe, Japan). Briefly, white blood cells count was performed using a semiconductor laser and flow cytometry, platelet count was performed by impedance and/or flow cytometry and the hemoglobin concentration was determined using sodium lauryl sulfate. Ferritin was determined in serum samples by chemiluminescent microparticle immunoassay using the automated clinical chemistry analyzer Alinity I (Abbott Laboratories, IL, US).

Statistical analysis

Results are expressed as mean ± standard error of the mean (SEM). Data were analyzed using Student's unpaired *t* test with one-tailed *p* value when comparing two groups. One-way ANOVA with unpaired Dunnett's post-hoc test was used for multiple comparisons with one factor, and two-way ANOVA with Sidak's post-hoc test was used for multiple comparisons with two factors. In all cases, a value of $p < 0.05$ was considered statistically significant. Statistical analysis was performed with the Prism 7.0 GraphPad Software.

Results

ER stress-induced UPR in human THP-1 monocytes

Under ER stress conditions, the UPR signaling pathway is activated to restore ER homeostasis, thus preserving cell survival, however, apoptotic cell death can be triggered by chronic stress [4, 5]. First, to characterize ER stress in human THP-1 monocytes, protein levels of UPR markers were analyzed in TM-treated cells by WB analysis, including p-eIF2α and ATF4 (mediators of the PERK UPR pathway), IRE1α and XBP1s (mediators of the IRE1α UPR pathway), GRP78 (the major ER-resident chaperone) and CHOP (a key ER stress-induced pro-apoptotic transcription factor). The levels of the above ER stress markers were assessed in a time-dependent manner (1–24 h) using 5 or 10 µg/mL TM, a well-established ER stress inducer. Protein levels of p-eIF2α and ATF4, as well as of IRE1α and XBP1s, significantly increased in THP-1 cells upon incubation with TM when compared with controls, indicating the activation of the PERK- and IRE1-mediated UPR pathways, respectively (Fig. 1A–D). More specifically, p-eIF2α levels were significantly enhanced after 1 and 4 h of TM treatment (Fig. 1A), which was followed by a significant rise of ATF4 content at 4 and 8 h (Fig. 1B). The upregulation of IREα was observed 8 and 24 h after TM exposure, whereas the augment of XBP1s protein levels was more evident at 4 and 8 h (Fig. 1C, 1D). In addition, a time- and dose-dependent increase in the levels of the ER-resident chaperone GRP78 occurred in TM-treated cells, and reached statistical significance at later time points, namely 8 and 24 h (Fig. 1E). Finally, levels of the pro-apoptotic factor CHOP were upregulated after 4 h of ER stress induction (Fig. 1F).

The above results demonstrate that TM-induced ER stress activates the UPR in human monocytes, namely the PERK and IRE1α signaling pathways, leading to the upregulation of pro-survival chaperones as well as pro-apoptotic factors.

ER stress response mechanisms in human THP-1 monocytes

Several proteins, such as PDI, ERO1α and Sigma-1 receptor (Sigma-1R), contribute to preserve ER function by regulating redox and Ca^{2+} homeostasis, however, ERO1α can potentiate apoptotic cell death during chronic ER stress [38–42]. Therefore, protein levels of PDI, ERO1α and Sigma-1R were evaluated by WB in THP-1 monocytes upon TM-induced ER stress (Fig. 2). A significant upregulation of the oxidoreductase ERO1α was observed at 8 h of treatment (Fig. 2B), in the absence of PDI alterations (Fig. 2A). A slight time-dependent increase of Sigma-1R protein levels, which was more pronounced after 4 and 8 h, was also detected under these conditions (Fig. 2C).

These results suggest that immune cells trigger adaptive responses to ER stress to preserve redox and Ca^{2+} homeostasis and thus cell survival, but that these adaptations occur concomitantly with activation of pro-apoptotic mechanisms that can involve upregulation of proteins, such as ERO1α,

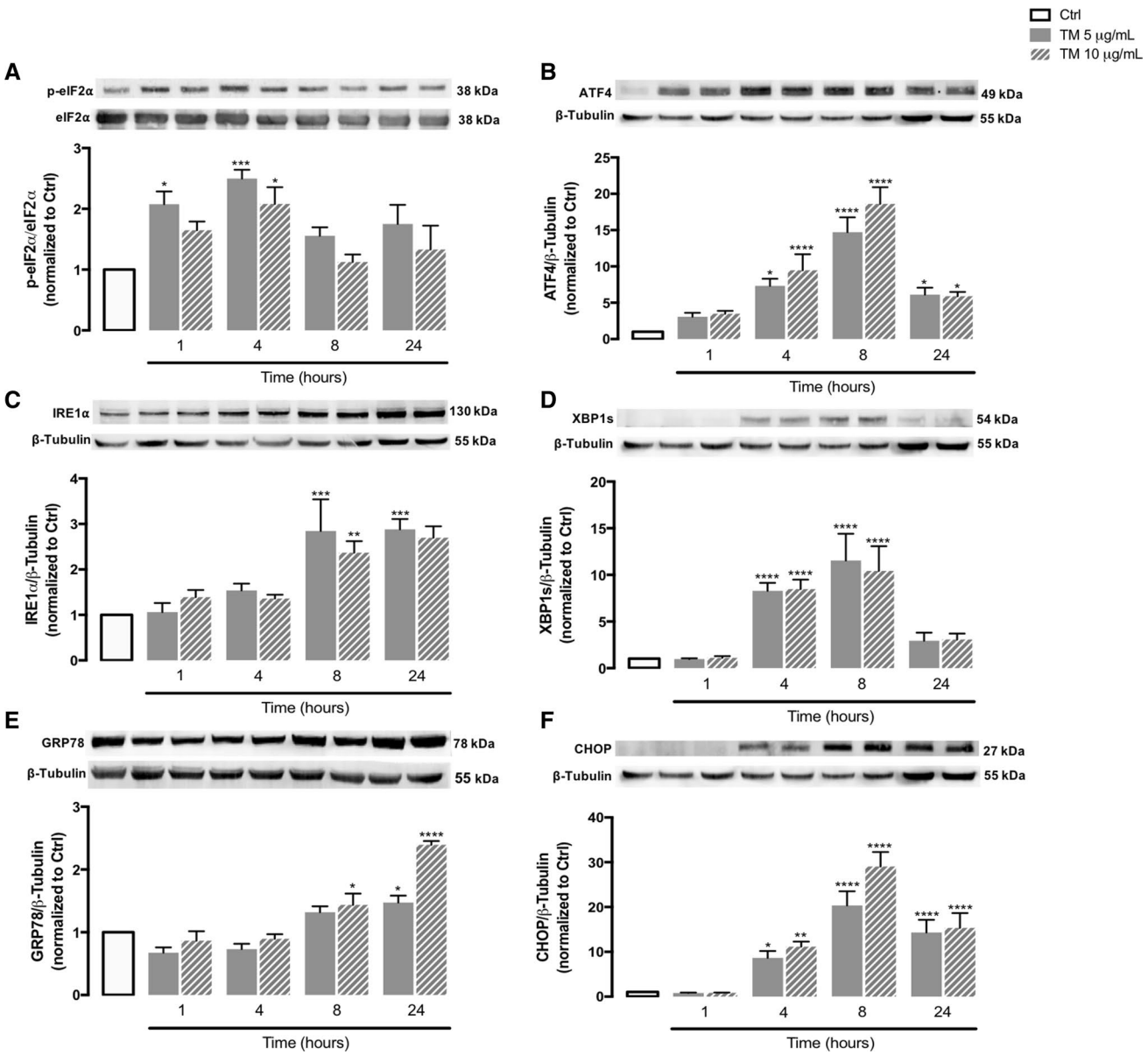

Fig. 1 ER stress-induced UPR in tunicamycin-treated human THP-1 monocytes. Protein levels of markers of ER stress-induced UPR, namely p-eIF2α (**A**), ATF4 (**B**), IRE1α (**C**), XBP1s (**D**), GRP78 (**E**) and CHOP (**F**) were quantified by WB in total cellular extracts obtained from human THP-1 monocytes treated with 5 or 10 μg/mL tunicamycin (TM) during the indicated time periods (1–24 h). β-Tubulin I was used to control protein loading and to normalize the levels of the protein of interest. For p-eIF2α quantification, total eIF2α was used as a protein loading control. Results were calculated relatively to control values and represent the mean ± SEM of at least three independent experiments. Statistical significance between control (untreated cells) and TM-treated cells was determined using the one-way ANOVA test, followed by the Dunnett's post hoc test: $*p<0.05$; $**p<0.01$; $***p<0.001$, $****p<0.0001$

that translocate to MAMs upon chronic stress and can promote excessive ER-mitochondria Ca^{2+} transfer.

ER morphology and ER-mitochondria contacts under stress conditions in human THP-1 monocytes

TM-treated monocytes were analyzed by transmission electron microscopy (TEM) and compared with control cells to unveil the alterations caused by ER stress in the morphology of this organelle with a special focus on its dilation, as well as on the number of ER-mitochondria contact sites

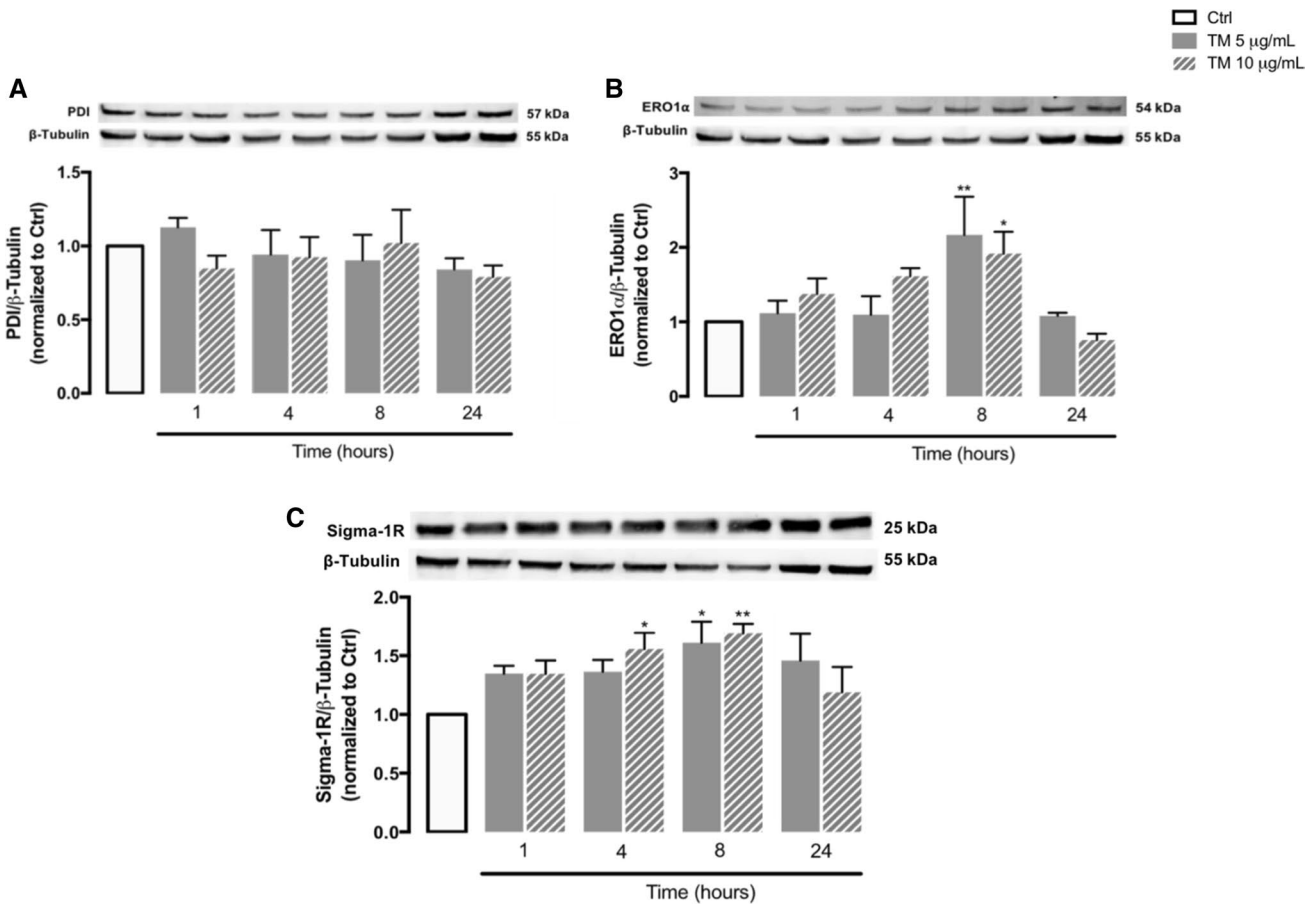

Fig. 2 Stress response mediators under ER stress conditions in human THP-1 monocytes. Protein levels of PDI (**A**), ERO1α (**B**) and sigma-1R (**C**) were quantified by WB in total cellular extracts obtained after treatment of THP-1 cells with 5 or 10 µg/mL tunicamycin (TM), during the indicated time periods (1–24 h). β-Tubulin I was used as a control for protein loading and to normalize the levels of the protein of interest. Results were calculated relatively to control values and represent the mean ± SEM of at least three independent experiments. Statistical significance between control and TM-treated cells was determined using the one-way ANOVA test, followed by Dunnett's post hoc test: $*p < 0.05$, $**p < 0.01$

(Fig. 3). THP-1 monocytes exposed to TM exhibited an enhanced width of the ER relative to control cells (Fig. 3A, B). Concomitantly, TM-induced ER stress increased the number of ER-mitochondria contacts per mitochondria, both contacts ≤100 nm (Fig. 3C, D), as well as close ER-mitochondria contacts ≤15 nm that are classified as MAMs (Fig. 3C, E).

These findings indicate that the response to stress triggered by TM in human monocytes modulates the coupling between ER and mitochondria, as demonstrated by increased ER-mitochondria contacts sites at MAMs.

Mitochondrial mass and number in human THP-1 monocytes upon ER stress

To evaluate the role of ER stress on mitochondria content, the protein levels of several mitochondrial mass markers were evaluated by WB in stressed THP-1 cells, namely ND1, MTCO1 and TOM20, and the activity of citrate synthase was analyzed. ND1 and MTCO1 are subunits of the complex I and IV of the mitochondrial electron respiratory chain, respectively [43], and T0M20 is a subunit of the mitochondrial import receptor TOM, which is located in the outer mitochondria membrane and plays an essential role in the specificity of protein import into mitochondria [44]. Citrate synthase is the enzyme that catalyzes the first reaction of the Krebs cycle [45]. Additionally,

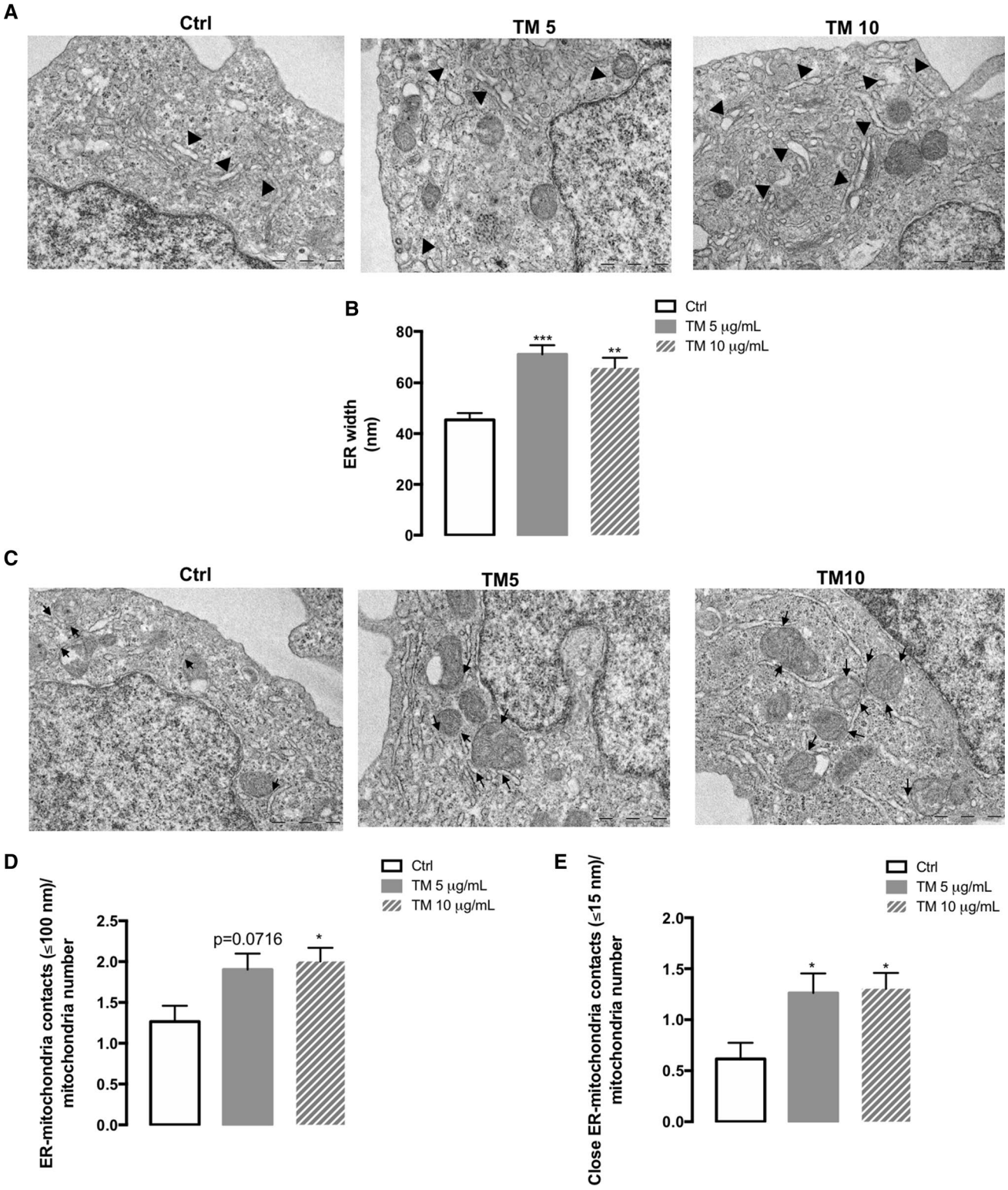

protein levels of TFAM, a mitochondrial transcription factor that plays an important role in the transcription and replication of mtDNA, were analyzed as a marker of mitochondrial biogenesis [46].

No significant differences in the protein levels of TOM20 (Fig. 4A), MTCO1 (Fig. 4B), ND1 (Fig. 4C) and TFAM (Fig. 4D), as well as in the activity of citrate synthase (Fig. 4E) were observed between untreated and treated cells, suggesting preservation of mitochondria

◂**Fig. 3** ER morphology and ER-mitochondria contacts under ER stress conditions in human THP-1 monocytes. Alterations in width of ER and in the number of ER-mitochondria contacts due to ER stress were monitored by TEM in human THP-1 monocytes treated with 5 or 10 µg/mL TM for 8 h and compared with untreated cells. (**A**) Representative images of dilated ER (arrowhead); (**B**) ER width expressed in nm; (**C**) Representative images of ER-mitochondria contacts (arrow); (**D**) Number of ER-mitochondria contacts (≤ 100 nm) normalized to mitochondria number; (**E**) Number of close ER-mitochondria contacts (≤ 15 nm) normalized to mitochondria number. Results represent the mean ± SEM of 4–5 images per cell obtained from 5 cells analyzed per condition. Statistical significance between control (untreated cells) and TM-treated cells was determined using the one-way ANOVA test, followed by the Dunnett's post hoc test: *$p < 0.05$, **$p < 0.01$, *** $p < 0.001$

mass/number in stressed THP-1 cells. These observations were further supported by data from TEM (Fig. 3) reporting no alterations in the number of mitochondria between stressed and non-stressed THP-1 cells (Fig. 4F).

Taken together, our results suggest that ER stress does not affect mitochondrial mass and number in human THP-1 monocytes.

Mitochondrial dynamics in human THP-1 monocytes upon ER stress

The transfer of stress signals between ER and mitochondria at the MAM's interface affects mitochondrial morphology [47]. To assess the impact of ER stress on mitochondrial dynamics, the levels of Mfn2, a protein that modulates mitochondria fusion [48] and is also responsible for ER-mitochondria tethering [49], were evaluated by WB in stressed THP-1 cells. A significant upregulation of Mfn2 was observed in response to ER stress, particularly after 4 and 8 h of TM treatment (Fig. 5A). In addition, the levels of the phosphorylated form of DRP1, which is a regulator of mitochondrial fission, were also investigated and a time-dependent decline in p-DRP1 levels occurred in TM-treated cells in comparison with controls (Fig. 5B). These results suggest an imbalance on mitochondrial dynamics towards mitochondrial fusion in monocytes in response to stress.

Mitochondrial redox status under stress conditions in human THP-1 monocytes

Prolonged ER stress has been related to oxidative stress, which is the imbalance between the production of ROS and antioxidant defenses, and can ultimately lead to cell death [50]. To investigate the effect of ER stress on mitochondrial redox status, the activity of aconitase, an enzyme from the tricarboxylic acid cycle that is sensitive to ROS, and of the mitochondrial antioxidant enzyme superoxide dismutase 2 (SOD2), were measured in both TM-treated THP-1 monocytes and control cells. Aconitase activity was not different between untreated and treated cells (Fig. 6A). On the other hand, increased activity of SOD2 (mitochondrial SOD isoform), concomitantly with a decrease in the activity of SOD1 (cytosolic SOD isoform), were observed in THP-1 cells upon 4 h of ER stress induction (Fig. 6B).

The above findings support that activation of the mitochondrial antioxidant SOD2 enzyme might represent an adaptive strategy to cope with ER stress and avoid the accumulation of deleterious ROS in the mitochondria to preserve cell survival.

Mitochondrial calcium uptake and mitochondrial membrane potential during ER stress in human THP-1 monocytes

In response to mild/early ER stress, mitochondrial Ca^{2+} uptake can be stimulated to preserve cell metabolism and provide energetic substrates to sustain an adaptive cellular response. However, under severe/prolonged ER stress conditions, excessive Ca^{2+} influx into mitochondria might collapse mitochondrial metabolism, promoting mitochondrial membrane depolarization and activation of deleterious signaling pathways [51].

Because of technical limitations, analysis of Ca^{2+} transfer at MAMs to evaluate functional ER-mitochondria coupling was not possible in THP-1 monocytes, but information on mitochondrial Ca^{2+} uptake was provided by using the Rhod-2AM fluorescent probe. Fluorescence values were determined in both basal and stimulation conditions using thapsigargin to induce ER Ca^{2+} depletion. Thapsigargin is a SERCA Ca^{2+}-ATPase inhibitor, resulting in Ca^{2+} depletion from internal stores due to stimulation of ER Ca^{2+} release [52]. Our data, which represents the difference between the highest post-thapsigargin fluorescence value and the mean of resting fluorescence levels, indicate that in response to TM-induced ER stress, mitochondrial Ca^{2+} content was significantly increased at 4 h and then decreased at 8 h (Fig. 7A). This decrease in mitochondrial Ca^{2+} uptake at 8 h can arise from the depolarization of mitochondrial membrane that was triggered 4 h after stress induction in human monocytes (Fig. 7B), which in turn might arise from the accumulation of Ca^{2+} within the mitochondrial lumen.

The above results demonstrate that ER stress induction enhances Ca^{2+} influx into mitochondria and leads to mitochondrial membrane depolarization, suggesting that ER stress triggers mitochondrial dysfunction in innate immune cells.

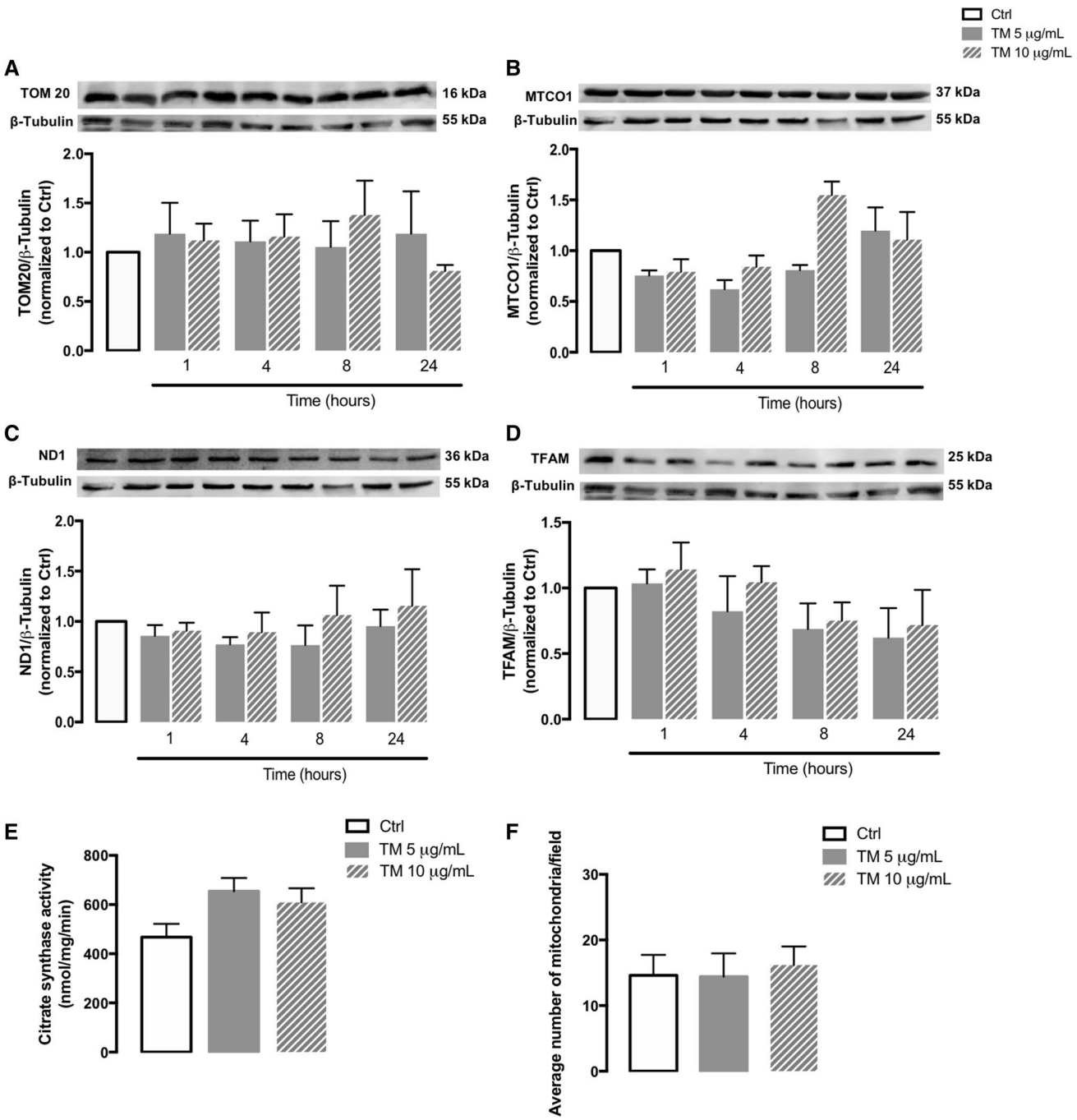

Fig. 4 Mitochondrial mass and number in human THP-1 monocytes upon ER stress. Protein levels of TOM20 (**A**), MTCO1 (**B**), ND1 (**C**) and TFAM (**D**) were quantified by WB in total cellular extracts obtained after incubation of THP-1 cells with 5 or 10 μg/mL TM, during the indicated time periods (1–24 h). β-Tubulin I was used as a control for protein loading and to normalize the levels of the protein of interest. Results were calculated relatively to control values and represent the mean ± SEM of at least three independent experiments. Mitochondrial citrate synthase activity (**E**) was evaluated in total cell lysates obtained after incubation of THP-1 cells with 5 or 10 μg/mL TM for 8 h. Results were expressed in nmol/mg/min and represent the mean ± SEM of at least three independent experiments. The number of mitochondria (**F**) was also determined in human THP-1 monocytes treated with 5 or 10 μg/mL TM for 8 h and compared to untreated cells, by analyzing TEM images (Fig. 3). Statistical significance between control and TM-treated cells was determined using the one-way ANOVA test, followed by Dunnett's post hoc test

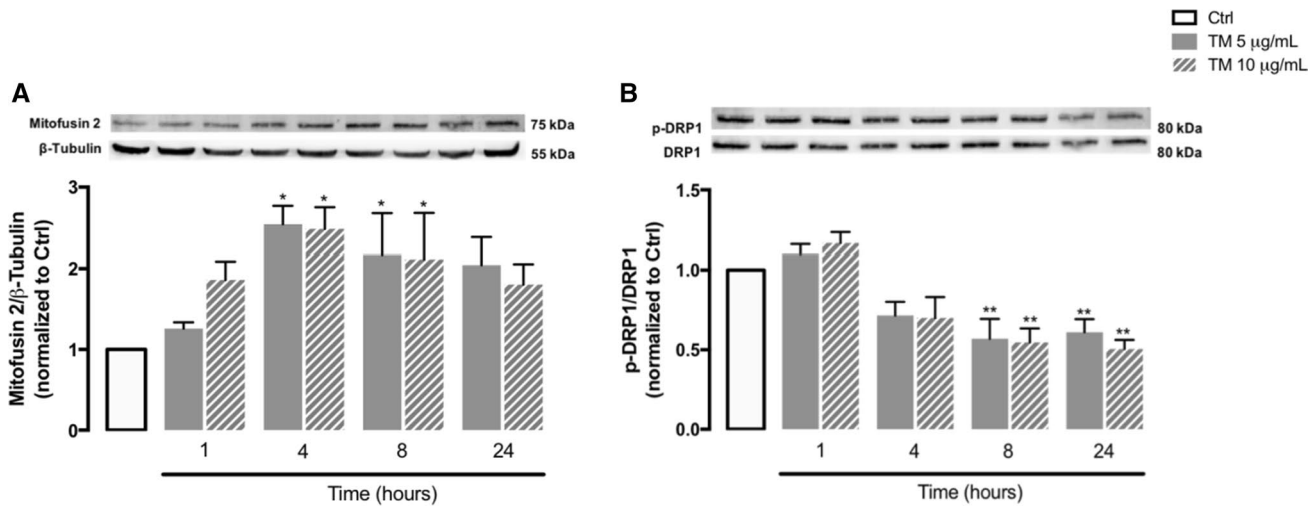

Fig. 5 Mitochondrial dynamics in human THP-1 monocytes upon ER stress. Protein levels of Mfn2 (**A**) and p-DRP1 (**B**) were quantified by WB in total cellular extracts obtained after incubation of THP-1 cells with 5 or 10 μg/mL TM, during the indicated time periods (1–24 h). β-Tubulin I was used as a control for protein loading and to normalize the levels of the protein of interest. Total DRP1 was used to normalize p-DRP1 levels. The membrane incubated with Sigma-1R antibody was re-probed with Mfn2 antibody and finally, re-probed with the anti-β-Tubulin I antibody. The membrane incubated with p-DRP1 antibody was then re-probed with total DRP1 antibody. Results were calculated relatively to control values and represent the mean ± SEM of at least three independent experiments. Statistical significance between control and TM-treated cells was determined using the one-way ANOVA test, followed by Dunnett's post hoc test: $*p<0.05$, $**p<0.01$

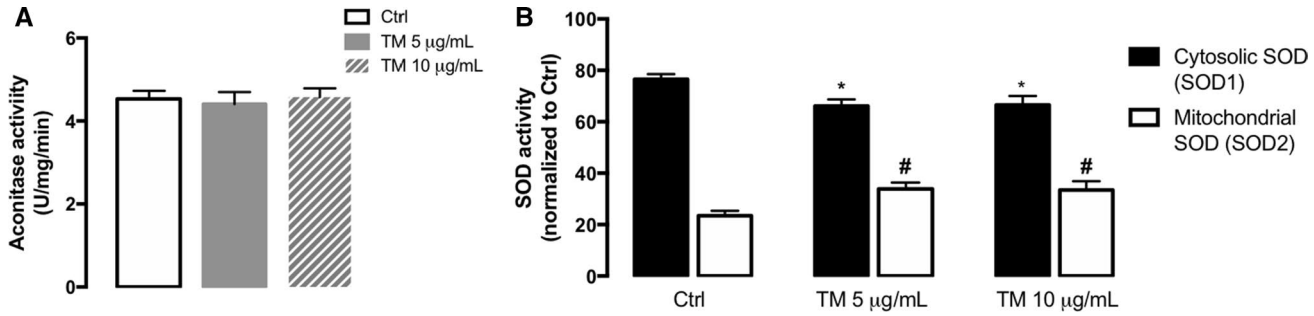

Fig. 6 Redox status under stress conditions in human THP-1 monocytes. Activity of the ROS-sensitive aconitase (**A**) was evaluated in total cell lysates obtained after incubation of THP-1 cells with 5 or 10 μg/mL TM for 8 h. Results were expressed as U/mg/min and represented as mean ± SEM of three independent experiments. Statistical significance of differences between control and treated cells was determined using the one-way ANOVA test, followed by Dunnett's post hoc test. The activity of cytosolic SOD1 and mitochondrial SOD2 (**B**) was analyzed by using a commercial kit in total lysates obtained from cells treated with 5 or 10 μg/mL TM for 4 h. Results were normalized to untreated cells and represented as mean ± SEM of three independent experiments. Statistical differences between control and TM-treated cells were obtained with the two-way ANOVA test, followed by Sidak's post hoc test: SOD1 ($*p<0.05$) and SOD2 ($^{\#}p<0.05$) activities

NLRP3 inflammasome activation in THP-1 monocytes exposed to ER stress

After demonstrating that ER stress modulates MAM's structure and function in peripheral human monocytes, we further investigated its role in NLRP3 inflammasome activation, which is described as a two-step process that requires two signals [20]. First, protein levels of NLRP3, pro-IL-1β and ASC were evaluated by WB in LPS-primed monocytes in the presence or absence of 10 μg/mL TM for 8 h and compared to control cells. An increase in the protein levels of NLRP3 and pro-IL-1β (Fig. 8A, B), in the absence of changes in ASC content (Fig. 8C), was detected in cells treated with LPS or LPS plus TM, suggesting that TM-induced ER stress doesn't act as a first (priming) signal for NLRP3 activation in human monocytes. Then, IL-1β secretion was quantified as a readout of NLRP3 inflammasome activation. It was observed that ER stress

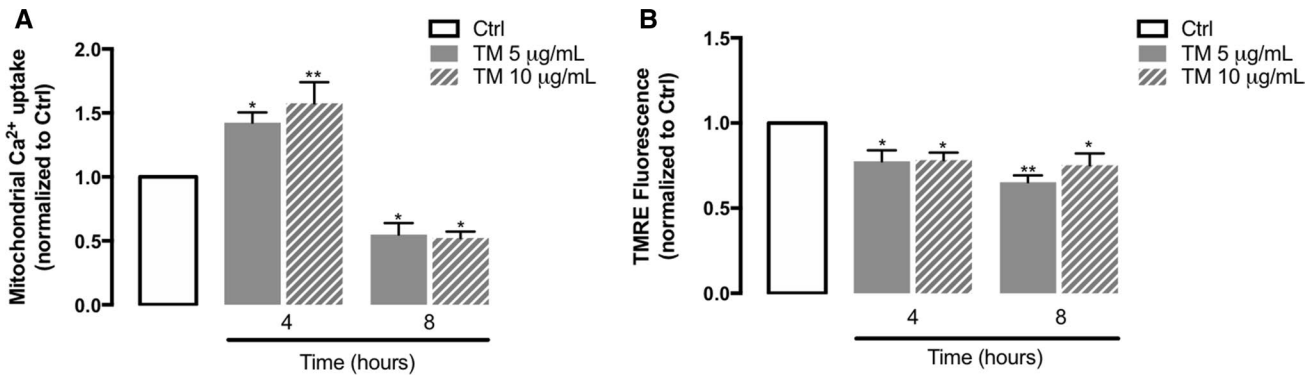

Fig.7 Mitochondrial calcium uptake and mitochondrial membrane potential under ER stress conditions in human THP-1 monocytes. Ca^{2+} influx into mitochondria was measured in THP-1 cells treated with 5 or 10 μg/mL TM for 4 or 8 h with the fluorescent probe Rhod-2/AM, before and after thapsigargin-induced ER Ca^{2+} depletion. Results were expressed by the difference between the highest post-thapsigargin value and the mean of baseline levels (**A**). Alterations in mitochondrial membrane potential (**B**) were measured using the TMRE fluorescent probe in THP-1 monocytes treated with 5 or 10 μg/mL TM for 4 or 8 h. Results were calculated relatively to control values and represent the mean ± SEM of three independent experiments. Statistical differences between control and TM-treated cells were obtained with the one-way ANOVA test, followed by the Dunnett's post hoc test: $*p < 0.05$; $**p < 0.01$

per se was not able to activate the NLRP3 inflammasome in human monocytes since the levels of IL-1β secreted by TM-treated cells were undetectable. Therefore, THP-1 monocytes were primed with LPS before ER stress induction for 8 h. As a positive control, the canonical NLRP3 activators LPS plus ATP were used [53] (Fig. 8D). IL-1β release increased by about 100-fold relatively to control in cells treated with LPS alone and an additional increase of about 100-fold was observed in cells primed with LPS and then treated with TM, demonstrating that ER stress activates the NLRP3 inflammasome in human primed THP-1 monocytes.

These findings strongly suggest that although ER stress doesn't work as a signal 1 (priming step), it can efficiently act as a second signal (activation step) to trigger NLRP3 inflammasome activation, and subsequent IL-1β release in human innate immune cells.

Role of Ca^{2+} on ER stress-induced NLRP3 activation in human THP-1 monocytes

After demonstrating that ER stress activates the NLRP3 inflammasome in human monocytes, the next step was to disclose the molecular mechanisms underlying its activation. Since ER stress was shown to increase ER-mitochondria contacts and promote early Ca^{2+} influx into mitochondria, it was tested the hypothesis that Ca^{2+} can play a role in ER stress-induced NLRP3 activation in innate immune cells. For that purpose, IL-1β levels secreted by primed THP-1 monocytes treated with TM for 8 h were measured in the presence or absence of Ru360, an inhibitor of the mitochondrial calcium uniporter (MCU), or xestospongin C (Xest C), a selective inhibitor of ER IP_3R-associated Ca^{2+} channels. A significant decrease of IL-1β levels was observed in LPS-primed THP-1 cells treated with 10 μg/mL TM either in the presence of Ru360 or Xest C (Fig. 9A, B). Additionally, to further evaluate the role of ROS on ER stress-induced NLRP3 activation in human THP-1 monocytes, we also tested the effect of the antioxidant NAC on IL-1β secretion in TM-treated monocytes (Fig. 9C) and it was ineffective showing that ROS are not implicated in NLRP3 activation on these cells. The susceptibility of THP-1 human monocytes towards ER stress was assessed using the viability resazurin assay in cells treated with 5 or 10 μg/mL TM during 4, 8 and 24 h. It was shown that both TM doses slightly affected cell viability after 8 h of exposure, which was decreased by approximately 30% at 24 h (Fig. 9C).

These results suggest that ER stress-induced NLRP3 inflammasome activation in peripheral immune cells occurs in a Ca^{2+}-dependent, and ROS-independent manner, and involves both ER Ca^{2+} release through the IP_3R and early Ca^{2+} influx into mitochondria by the MCU, later compromising cell survival.

NLRP3 inflammasome activation in BV2 microglia cells exposed to ER stress

After disclosing ER stress as an activator of the NLRP3 inflammasome in the peripheral innate immune system, we further addressed whether a similar event also occurs in innate immune cells from the central nervous system (CNS). For that, the role of ER stress on NLRP3 inflammasome activation was evaluated in BV2 microglial cells exposed to the ER stress inducer brefeldin A (BFA). UPR induction was evaluated by determining the protein levels of the ER-resident GRP78 chaperone, and NLRP3 inflammasome

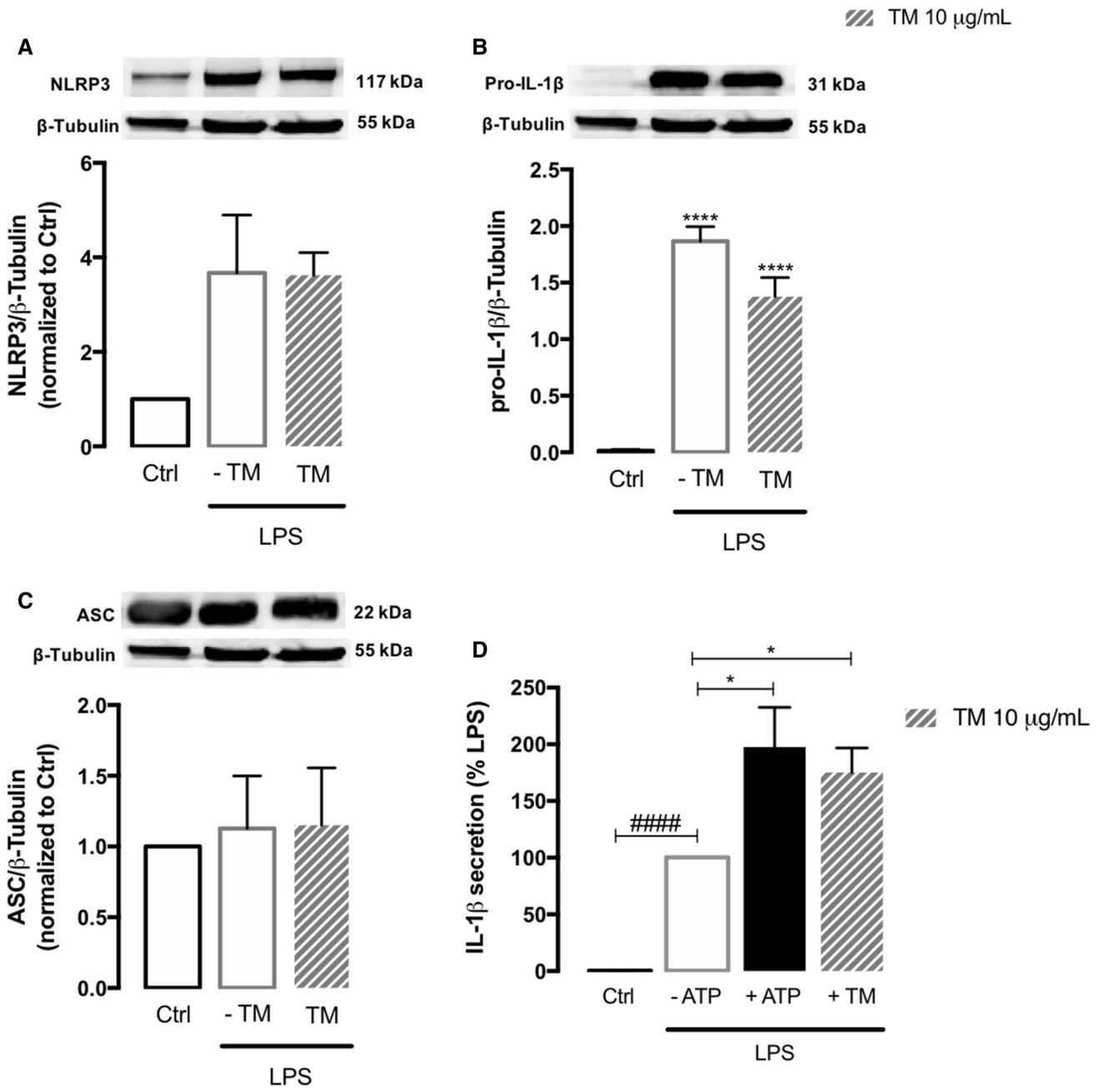

Fig. 8 NLRP3 inflammasome activation in human monocytes exposed to ER stress. Protein levels of NLRP3 (**A**), pro-IL-1β (**B**) and ASC (**C**) were quantified by WB in total extracts from THP-1 monocytes incubated in the presence or absence of 10 μg/mL TM for 8 h, upon priming with LPS (1 μg/mL) during 24 h. β-Tubulin I was used as a loading control to normalize the levels of the protein of interest. Results were calculated relatively to control values, with exception of pro-IL-1β, and represent the mean ± SEM of at least three independent experiments. Statistical significance between control and TM-treated cells was determined using the one-way ANOVA test, followed by Dunnett's post hoc test: ****$p < 0.0001$. Levels of secreted IL-1β were quantified by an ELISA assay in supernatants of THP-1 cells treated with 1 μg/mL LPS alone (24 h), or with LPS (24 h) and then with 10 μg/mL TM for the last 8 h. Cells primed with 1 μg/mL LPS for 24 h and then exposed to 5 μM ATP for 30 min were used as a positive control for NLRP3 activation. Results were calculated relatively to LPS-treated cells and represent the mean ± SEM of at least three independent experiments. Statistical significance between LPS and control conditions (Ctrl), in the absence of treatments, was determined by student's *t*-test ($^{\#\#\#\#}p < 0.0001$), and between LPS, LPS plus ATP and LPS plus TM was determined using the one-way ANOVA test, followed by Dunnett's post hoc test: *$p < 0.05$

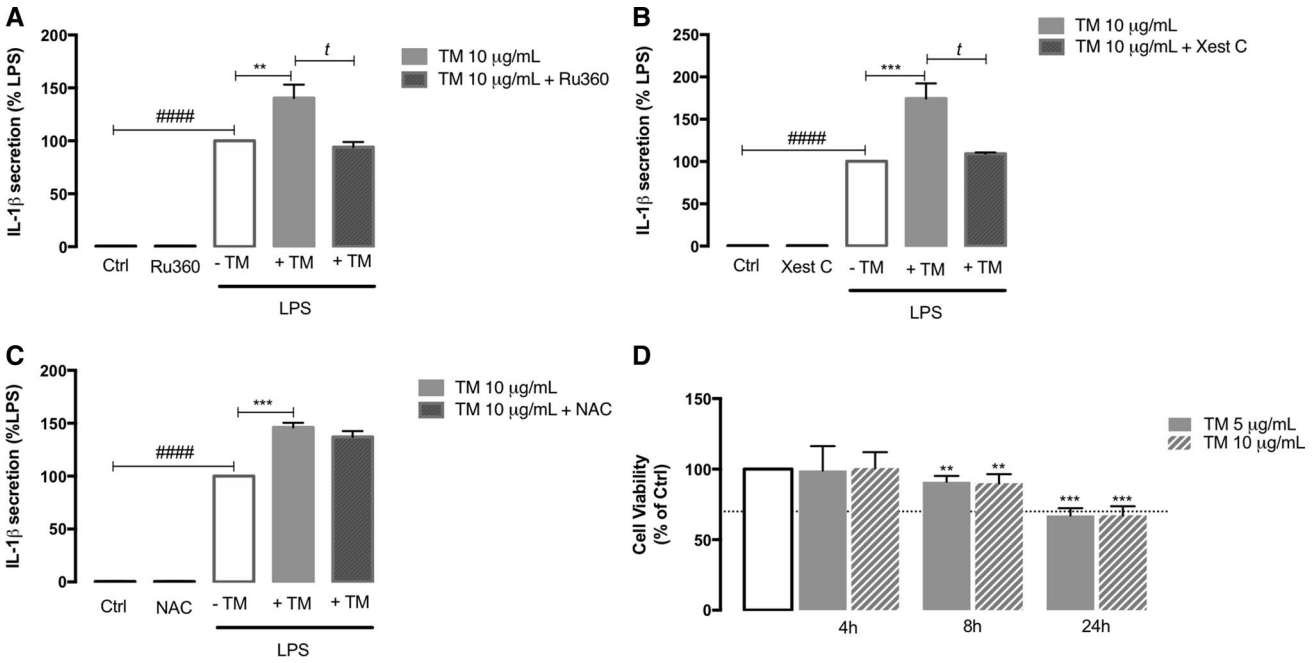

Fig. 9 Role of Ca^{2+} on ER stress-induced NLRP3 activation in THP-1 monocytes and susceptibility towards ER stress. By using an ELISA assay, IL-1β secretion was analyzed in supernatants obtained from THP-1 cells primed with 1 μg/mL LPS during 24 h and then treated with 10 μg/mL TM for 8 h in the presence or absence of 10 μM Ru360 (**A**), or 1 μM Xest C (**B**), or 5 mM NAC (**C**) which were pre-incubated during 1 h. Results were calculated relatively to LPS-treated cells and represent the mean ± SEM of at least three independent experiments. Statistical analysis: *t*-test was used for comparisons between Ctrl and LPS ($^{\#\#\#}p < 0.001$), LPS plus TM and LPS ($^{**}p < 0.01$ or $^{***}p < 0.001$), LPS plus TM plus Xest C and LPS plus TM ($^{t}p < 0.05$), and LPS plus TM plus Ru360 and LPS plus TM ($^{t}p < 0.05$). Susceptibility of THP-1 cells to ER stress induced by TM (5 or 10 μg/mL) exposure during 4, 8 or 24 h was assessed by the resazurin assay (**D**). Results represent the mean ± SEM of at least three independent experiments and were calculated relatively to control values (untreated cells). Statistical significance between control and treated cells was determined using the one-way ANOVA test, followed by Dunnett's post hoc test: $^{**}p < 0.01$; $^{***}p < 0.001$

activation was analyzed by measuring the protein levels of NLRP3 and pro-IL-1β, as well as IL-1β secretion. BFA upregulated GRP78 levels when compared to the control condition, which reached statistical significance in microglia cells treated with 10 μM BFA (Fig. 10A). Besides that, treated BV2 microglia cells exhibited higher protein levels of NLRP3 (Fig. 10B) and pro-IL-1β (Fig. 10C), as well as a significant increase of secreted IL-1β levels upon LPS priming in comparison with control cells (Fig. 10D). Indeed, an increase in IL-1β secretion of about 250-fold was found in BV2 cells treated with 10 μM BFA when compared with LPS-treated cells. Furthermore, levels of IL-1β secreted by primed cells treated with 2 μM BFA showed a slight increase, although the augment did not reach statistical significance.

These results strongly suggest that ER stress not only activates the NLRP3 inflammasome in peripheral innate immune cells but also promotes its activation in CNS-resident microglia.

Pro-inflammatory status and NLRP3 inflammasome activation under ER stress conditions in bipolar disorder (BD) monocytes

After demonstrating that ER stress activates the NLRP3 inflammasome, promoting the release of pro-inflammatory IL-1β, in both peripheral and central innate immune systems, the modulation of NLRP3 inflammasome activation by ER stress was also investigated in patients with BD diagnosis versus healthy controls. Indeed, the pathophysiology of BD, which is a chronic and cyclic mental illness characterized by mood swings, has been associated with compromised ER stress response, mitochondrial dysfunction and changes in innate immunity [54–56]. This was a proof-of-concept study with a reduced number of participants from each group. The variability inter-donors, as well as the low yield of monocytes isolation from peripheral blood represented major limitations to the number of parameters analyzed.

First, several biochemical markers of inflammation were monitored in the blood samples from BD patients and controls after written informed consent. Although data from Table 1 did not show statistical differences in inflammatory

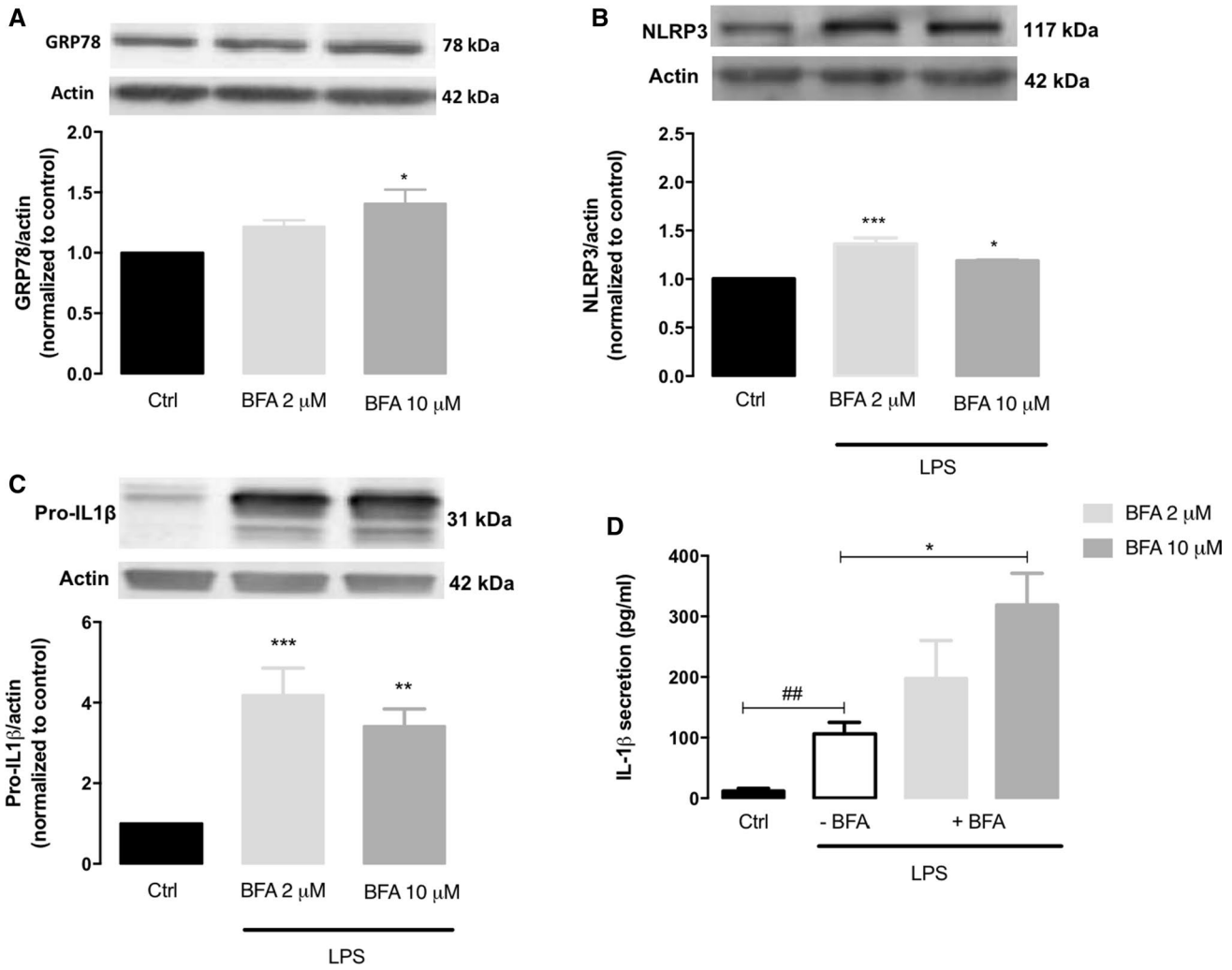

Fig. 10 NLRP3 inflammasome activation in microglia cells exposed to ER stress. Protein levels of GRP78 (**A**) were quantified by WB in total extracts obtained after treatment of BV2 cells with 2 or 10 μg/mL brefeldin A (BFA) for 6 h. NLRP3 (**B**) and pro-IL-1β (**C**) content was also quantified by WB in total extracts of BFA-treated BV2 cells upon LPS priming (3 h). Actin was used as a protein loading control to normalize the levels of the protein of interest. Results were calculated relatively to control values and represent the mean ± SEM of at least three independent experiments. Statistical significance between control and BFA-treated cells and between control and LPS plus BFA cells was determined using the one-way ANOVA test, followed by the Dunnett's post hoc test: $*p<0.05$, $**p<0.01$, $***p<0.001$. Secreted IL-1β levels (**D**) were measured using an ELISA assay in the supernatants collected from BV2 microglia cells treated with 300 ng/mL LPS alone (3 h), or primed with LPS and then incubated with BFA 2 or 10 μg/mL) for 6 h. Results represent the mean ± SEM of at least three independent experiments. Statistical significance between LPS and control conditions (Ctrl), in the absence of treatments, was determined by student's *t*-test ($^{\#\#}p<0.01$), and between LPS and LPS plus BFA cells was determined using the one-way ANOVA test, followed by the Dunnett's post hoc test: $*p<0.05$

markers between both groups of participants, a basal pro-inflammatory status is suggested to occur in BD patients. In comparison with controls, patients exhibited higher levels of leukocytes namely neutrophils, as well as ferritin. Moreover, an increase in the number of platelets was detected in BD individuals compared to controls, as well as in the circulatory innate and adaptive immune cells such as monocytes and lymphocytes, respectively. BD-associated inflammatory status is further supported by the higher yield of monocytes (20%) isolated from PBMCs fraction from BD patients when compared to controls.

Then, the activation of the NLRP3 inflammasome was assessed in monocytes derived from BD patients and healthy controls by analyzing the protein levels of NLRP3 and pro-IL-1β and by quantifying the levels of IL-1β secreted after treatment with the ER stress inducer TM for 32 h (Fig. 11). Basal levels of NLRP3 (Fig. 11A) and pro-IL-1β (Fig. 11B) were not different between BD and control monocytes. However, in response to ER stress, the protein levels of NLRP3

Table 1 Clinical parameters on healthy individuals (controls) versus BD patients

Clinical parameters	Ctrl	BD patients
Age (years)	28.20 ± 2.48	27.80 ± 2.20
Leukocytes ($\times 10^9$/L)	6.72 ± 0.34	8.04 ± 1.37
Neutrophils ($\times 10^9$/L)	3.88 ± 0.35	4.92 ± 1.05
Lymphocytes ($\times 10^9$/L)	1.94 ± 0.36	2.28 ± 0.31
Monocytes ($\times 10^9$/L)	0.52 ± 0.05	0.68 ± 0.08
Ferritine (ng/mL)	171.40 ± 61.64	215.60 ± 55.44
Platelets ($\times 10^9$/L)	197 ± 19.71	248.60 ± 24.10
Protein C reactive (mg/dL)	0.20 ± 0.12	0.22 ± 0.12

were significantly higher in BD than in control monocytes (Fig. 11C). Accordingly, under ER stress conditions, there was a significant increase in IL-1β secretion by BD patients-derived monocytes, which was not observed in control monocytes (Fig. 11D).

Interestingly, these results demonstrate that although under basal conditions the activity of NLRP3 inflammasome is not different between BD patients and healthy controls, the susceptibility of the immune system towards ER stress is affected, with a significant activation of this inflammasome observed in BD patients-derived monocytes upon ER stress, which reinforces the presence of a pro-inflammatory status in BD.

Discussion

Over the past years, disturbances in innate immunity have been implicated in several human pathological conditions such as cancer, metabolic, neurodegenerative, as well as psychiatric diseases [57]. A close interaction between immune responses and ER stress has been reported, however, the molecular basis of this relationship remains largely unexplored [58]. Concomitantly, the growing knowledge of close ER-mitochondria junctions, the so-called MAMs, allowed to disclose their structure including the identification of tethering proteins, and function, namely their role as key mediators of ER stress and inflammatory responses [13, 15].

The present study was designed to investigate the ER stress-MAMs-inflammation axis in peripheral and central innate immune cells, as well as to address its role in BD pathophysiology by using a patient-derived cell-based model. The major findings obtained using THP-1 human monocytes demonstrate that ER stress interferes with MAMs composition and function, and activates the NLRP3 inflammasome culminating in the secretion of the pro-inflammatory cytokine IL-1β, further supporting that this activation involves the communication between the ER and mitochondria. Similarly, ER stress-induced NLRP3 inflammasome activation was also observed in BV2 microglia cells. Finally, BD patients-derived monocytes were found more susceptible to ER stress-induced NLRP3 inflammasome activation in comparison to healthy controls.

First, ER stress was shown to be induced by TM in human THP-1 monocytic cell line, as demonstrated by the dose- and time-dependent alteration of several markers of the UPR, a conserved signaling pathway that restores ER homeostasis or triggers apoptotic cell death in response to stress. These findings are in accordance with results from previous studies demonstrating that TM is a pharmacological trigger of ER stress-induced UPR in cells from the innate immune system, such as macrophages [59]. The increase of p-eIF2α and ATF4 protein levels supports the activation of the UPR PERK branch in monocytes. ATF4 upregulation is a downstream event of eIF2α phosphorylation, which results from the dimerization and autophosphorylation of PERK. Therefore, eIF2α phosphorylation is an early event during ER stress conditions, whereas ATF4 expression occurs at later time points, after the decrease of global translation triggered by PERK-mediated eIF2α phosphorylation and preferential translation of some mRNAs [60]. Moreover, upregulation of IRE1α and XBP1s supports the activation of the UPR IRE1α branch in monocytes under stressful conditions. XBP1s is cleaved and activated by the dimerized and auto-phosphorylated IRE1α to increase ER quality control processes, namely the expression of chaperones such as GRP78 [61, 62]. In TM-treated THP-1 monocytes, non-phosphorylated IRE1α and GRP78 protein levels increased simultaneously. In fact, IRE1α pathway stabilizes the non-phosphorylated IRE1α through the formation of GRP78-IRE1α complex to promote adaptation to stressful stimuli [63]. Upon ER stress, ATF4 activation is followed by an increased translation of CHOP to reestablish protein synthesis, however, chronic CHOP expression can sensitize cells towards apoptosis [64, 65].

Proteins involved in the cellular response to stress were then evaluated in human monocytes, and it was found an increase in the levels of ERO1α, which acts together with PDI to regulate ER redox signaling, and also modulates IP_3R-mediated Ca^{2+} release [40]. Under prolonged stress, the ERO1α oxidoreductase is almost exclusively found at MAMs [66], where it promotes excessive Ca^{2+} flux towards mitochondria [67], which was shown to be a pro-apoptotic trigger under these conditions [68]. In macrophages exposed to ER stress, ERO1α-IP_3R pathway was shown to mediate Ca^{2+}-dependent apoptosis induced by CHOP, which acts as a transcriptional inducer of ERO1α [40]. Additionally, the upregulation of Sigma-1R, a MAM's resident chaperone, may represent an attempt of THP-1 cells to preserve cell survival in response to stress, as supported by previous studies showing that a rapid rise of Sigma-1R levels is triggered to inhibit ER stress-induced cell death [69]. Under stressful conditions, Sigma-1R is also able to interact with ER IP_3R receptors, stabilizing their structure and stimulating Ca^{2+}

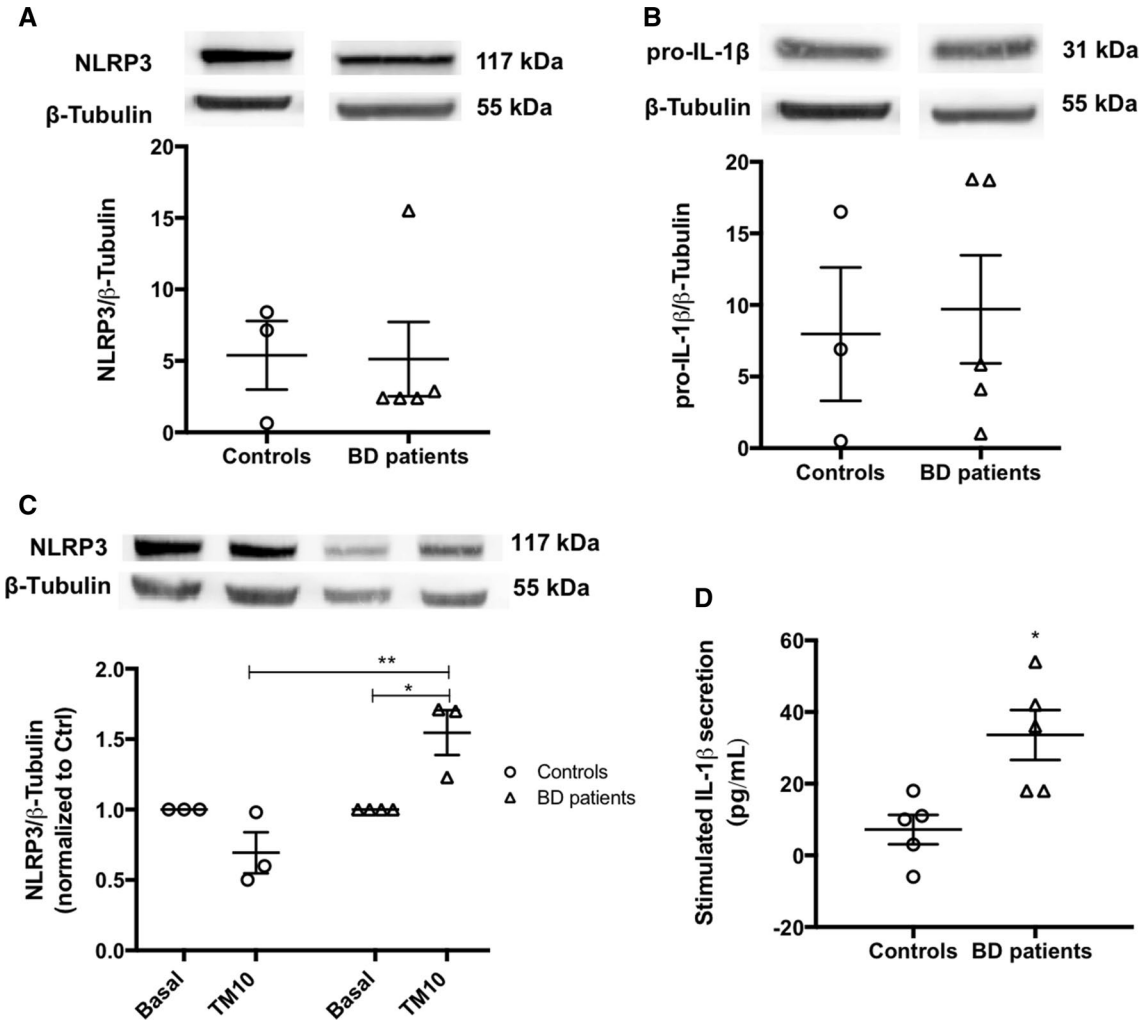

Fig. 11 NLRP3 inflammasome activation in BD-patient derived monocytes. Protein levels of NLRP3 (**A**) and pro-IL-1β (**B**) were quantified by WB in total extracts obtained from monocytes derived from healthy controls or BD patients under basal conditions. β-Tubulin I was used as a protein loading control to normalize the levels of the protein of interest. Data represent the mean ± SEM of results obtained in samples from 3–5 participants. Statistical significance between controls and BD patients was determined by Student's *t*-test. NLRP3 protein levels were also evaluated by WB in TM-stressed monocytes derived from BD patients and healthy controls (**C**). β-Tubulin I was used as a protein loading control to normalize the levels of the protein of interest. Results were calculated relatively to respective basal levels and represent the mean ± SEM of results obtained in samples from 3–5 participants. Statistical differences between basal and TM-treated cells within each experimental group, and between the two groups were obtained using the two-way ANOVA test, followed by the Tukey's post hoc test: (*$p < 0.05$) and (**$p < 0.01$). IL-1β levels (**D**) in supernatants from monocytes derived from healthy controls and BD patients treated with 10 μg/mL TM for 32 h, were quantified using an ELISA kit. Data represent the mean ± SEM of results obtained in samples from 5 participants. Statistical significance between controls and BD patients was determined by Student's *t*-test: *$p < 0.05$

influx into mitochondria, which is required to maintain ATP production through the electron transport chain [38, 42, 70]. Therefore, upregulation of the above MAM-resident chaperones indicates that ER stress modulates MAM's composition in human monocytes, and suggest an enhanced ER-mitochondria communication in response to stress, initially to preserve ATP synthesis but leading to cell death at later stages. This hypothesis was supported by results from TEM analysis showing that ER stress induction in THP-1 cells increases the number of ER-mitochondria contact sites per mitochondria, in particular, of close ER-mitochondria contacts that are defined as equal to or less than 15 nm. The increase of ER-mitochondria contacts in stressed THP-1 monocytes occurred in the absence of alterations of mitochondrial mass/number, as demonstrated by the absence of differences in the protein levels of several markers of mitochondrial mass such as MTCO1, ND1 and TOM20, as well as in the levels of TFAM, a biogenesis marker. The evidence that ER stress does not affect mitochondrial mass/number in these immune cells was further strengthened by

the similar activity of citrate synthase and mitochondria number between untreated and TM-treated monocytes. An increased ER-mitochondria coupling during early phases of ER stress has already been reported. Bravo and co-workers found a rise in the number of ER-mitochondria contact sites in HeLa cells treated with TM for 6 h, which stimulated mitochondrial Ca^{2+} uptake and metabolism. Additionally, these authors showed that in the absence of Mfn2, ER-mitochondria contacts were abolished and both mitochondrial Ca^{2+} uptake and oxygen consumption were impaired, leading to cell death [71].

Mfn2 is described as an important ER-mitochondria tethering protein that is located on both the surface of the OMM and the ER, thus regulating the inter-organelle proximity, as well as ER-mitochondria Ca^{2+} transfer [49]. However, how Mfn2 modulates ER-mitochondria juxtaposition is still controversial. The role of Mfn2 as a tether protein was purposed based on confocal microscopy data obtained in $Mfn2^{-/-}$ mouse embryonic fibroblasts (MEFs) that exhibited decreased ER-mitochondria colocalization and reduced mitochondrial Ca^{2+} uptake upon ER Ca^{2+} depletion [72, 73]. Furthermore, in $Mfn2^{-/-}$ mouse cardiomyocytes, a 30% reduction in the length of the close contacts between junctional sarcoplasmic reticulum and mitochondria was also reported [74]. Schneeberger and colleagues demonstrated the association between Mfn2 downregulation and decreased ER-mitochondria contacts in hypothalamic neurons from diet-induced obese mice [75]. The hypothesis that Mfn2 positively modulates ER-mitochondria coupling was also encouraged by findings showing that Mfn2 knockdown in muscle cells reduces mitochondrial Ca^{2+} uptake and by evidences that Mfn2-mediated mitochondrial Ca^{2+} uptake overcomes the low affinity of the mitochondrial Ca^{2+} uptake mediated by MCU [76]. By contrast, it was demonstrated in other studies that $Mfn2^{-/-}$ MEFs cells doubled the number of close contacts between the two organelles, which was rescued through Mfn2 re-expression [77, 78]. This evidence is in accordance with other studies showing that Mfn2 ablation or silencing increased ER-mitochondria close contacts and the efficiency of IP_3R-mediated Ca^{2+} transfer to mitochondria. Based on these results, the authors proposed a revised model for ER-mitochondria coupling in which Mfn2 works as a tethering antagonist, avoiding the excessive and toxic inter-organelle crosstalk [79]. In THP-1 monocytes, upregulation of Mfn2 upon ER stress is correlated with an increased number of ER-mitochondria close contacts, supporting that Mfn2 facilitates the tethering between ER and mitochondria in innate immune cells. Mfn2 is also a key mediator of mitochondrial fusion [80]. Accordingly, increased levels of Mfn2 during stress conditions are known to promote mitochondrial fusion in an attempt to compensate mitochondrial alterations, namely membrane depolarization, and preserve the functioning of these organelles [48]. Based on this, Mfn2 upregulation observed in TM-treated THP-1 monocytes could promote mitochondria fusion to ensure ATP production. However, excessive mitochondrial fusion can lead to the accumulation of damaged mitochondria [81]. A decrease in the protein levels of the p-DRP1 mitochondrial fission marker was observed in TM-treated THP-1 monocytes, supporting an unbalance between fusion/fission events in stressed innate immune cells. Mitochondrial fission is an event implicated in mitophagy that is required to decrease the size of mitochondria facilitating its entrance into autophagosomes and degradation in lysosomes [82]. Therefore, a decrease in fission events might anticipate the following scenarios: (1) removal of damaged mitochondria by mitophagy occurs through fission-independent mechanisms; (2) mitophagy occurs at low rates and dysfunctional mitochondria progressively accumulate in the cell, promoting stress, release of inflammatory cytokines, cell damage and death [48, 83].

MAMs function was also investigated in THP-1 monocytes under stressful conditions by the analysis of parameters such as mitochondrial redox status, membrane potential and Ca^{2+} signaling. Prolonged ER stress-induced UPR activation has been intimately associated with oxidative stress due to increased ROS production [50]. Recently, Knupp and colleagues have shown that ER stress triggers ROS production within mitochondria, and also demonstrated that ROS and cell death are increased by ER stress in cells with silenced IRE1α [84]. This link was further elucidated by previous studies showing that upregulation of ATF4 and CHOP transcription factors by chronic ER stress enhances protein synthesis and causes cell death due to ROS production caused by ATP depletion [85]. In the present study, the balance between ROS production and antioxidant defenses were assessed in THP-1 cells by measuring the activity of aconitase, a mitochondrial enzyme that is susceptible to the presence of ROS and is thus an oxidative stress marker, and also of the antioxidant SOD2 responsible for superoxide dismutation within the mitochondria. The unaltered aconitase activity in TM-treated cells in comparison with control cells indicates that under ER stress conditions the levels of ROS are not enhanced in the mitochondria, which can be justified by the activation of antioxidant defenses, namely SOD2. Indeed, in response to stress, the UPR PERK pathway promotes antioxidant responses mediated by ATF4 and NRF2, through the induction of antioxidant stress response genes such as those encoding SODs, heme oxygenase-1, glutathione transferase, and uncoupling mitochondrial protein 2, to prevent excessive accumulation of ROS and preserve normal mitochondria functioning [86].

Our findings showing upregulation of MAM-resident chaperones and enhanced ER-mitochondria contact sites suggest increased ER-mitochondria Ca^{2+} transfer under stress conditions in human monocytes, which would be in

accordance with other studies reporting Ca^{2+} transfer to mitochondria at the MAMs interface in response to chronic ER stress [87, 88]. Although several approaches to evaluate ER-mitochondria Ca^{2+} fluxes have been tested in THP-1 monocytes, none was able to be implemented due to the specific characteristics of this cell line. To overcome this limitation, we measured mitochondrial Ca^{2+} content in untreated or TM-treated THP-1 monocytes upon thapsigargin-induced ER Ca^{2+} release. Under these conditions, an increase in mitochondrial Ca^{2+} uptake was detected in THP-1 monocytes treated with TM for 4 h when compared to control cells. This increment in mitochondrial Ca^{2+} can be orchestrated by different cellular processes, such as bulk cytosolic Ca^{2+}, as well as the expression of MCU or mitochondrial Na^{+}/Ca^{2+} exchanger (NCLX). Cytosolic Ca^{2+} rise is followed by MCU activation to promote mitochondrial Ca^{2+} uptake to reestablish Ca^{2+} homeostasis [89]. In turn, Ca^{2+} content in mitochondria is regulated by MCU and NCLX. More specifically, MCU mediates the entry of Ca^{2+} into mitochondria, while NCLX controls mitochondrial Ca^{2+} extrusion. Thus, alterations in the expression of MCU/NCLX can explain changes in mitochondrial Ca^{2+} levels [90]. The mitochondrial permeability transition pore (mPTP) distinguishes between a permanent or a transient pore opening. The permanent pore opening involves the release of cytochrome c and the loss of the mitochondrial membrane potential, culminating in cell death. However, the opening of the mPTP also helps to modulate excessive mitochondrial Ca^{2+} content during physiological oscillations of cytosolic Ca^{2+} levels [91]. In THP-1 human monocytes, stressful conditions may compromise mPTP, leading to changes in mitochondrial Ca^{2+} content.

Interestingly, Carreras-Sureda and colleagues have recently found that IRE1α accumulates in MAM fractions in mouse embryonic fibroblasts (MEFs) under stress conditions, and is able to physically interact with IP_3Rs, resulting in enhanced mitochondrial Ca^{2+} uptake. These findings are in line with our data obtained in human THP-1 monocytes showing that IRE1α upregulation correlates with mitochondrial Ca^{2+} rise upon ER stress. Moreover, these authors also demonstrated that IRE1α regulates the abundance of IP_3Rs at MAMs, which are reduced in MAMs fractions isolated from IRE1α-deficient MEFs. In addition to confirm the occurrence of a transient rise of ATP levels, an early event during ER stress, it was shown that IRE1α is required to stimulate metabolism under these conditions since ATP production was almost suppressed in IRE1α-deficient cells [88].

The increase in mitochondrial Ca^{2+} content observed in THP-1 cells 4 h after TM exposure can be responsible for the loss of mitochondrial membrane potential. Indeed, a significant and sustained depolarization of the mitochondrial membrane potential was detected in monocytes upon TM-induced ER stress. Our data is corroborated by findings showing that the excessive ER-mitochondria Ca^{2+} transfer under chronic stress conditions can lead to mitochondrial Ca^{2+} overload and subsequent loss of membrane potential and activation of apoptotic cell death [92]. Curiously, at a later time point, namely 8 h of TM-induced ER stress, mitochondrial Ca^{2+} influx was significantly attenuated, which can arise from mitochondrial membrane depolarization. A recent study demonstrated that Ca^{2+} influx only occurs in mitochondria with preserved membrane potential [93], suggesting that prolonged membrane depolarization avoids Ca^{2+} uptake into mitochondria.

After demonstrating that ER stress modulates MAMs structure and function in innate immune cells, it was shown that it also induces NLRP3 inflammasome activation and subsequent release of the pro-inflammatory cytokine IL-1β. More detailed, it was found that although ER stress per se does not act as a signal 1 (priming step) for NLRP3 inflammasome activation, it works as a second signal (activation step), since TM treatment-induced IL-1β secretion in LPS-primed THP-1 cells. These findings are corroborated by previous results obtained by Menu and collaborators in other cells of the innate immune system, namely in LPS-primed human macrophages treated with TM [59]. However, while these authors demonstrated that ER stress-induced NLRP3 inflammasome activation is mediated by ROS production in macrophages, our findings suggest that in human monocytes it occurs in a ROS-independent manner. Indeed, the activity of the ROS-sensitive aconitase was not affected and the activity of the mitochondrial antioxidant superoxide dismutase (SOD2) was significantly stimulated in TM-treated THP-1 cells, suggesting that ROS accumulation is not induced by ER stress in human monocytes. Accordingly, the addition of the non-enzymatic antioxidant NAC was not able to prevent TM-induced NLRP3 inflammasome activation in LPS-primed THP-1 monocytes.

The assembly of the NLRP3 inflammasome at the MAMs platform under stress conditions strongly suggests that signals from mitochondria are responsible for its activation [94]. Based on that, we hypothesized that ER-mitochondria contacts may link ER stress to NLRP3 inflammasome activation in innate immune cells. Our findings showed that TM-induced IL-1β release in LPS-primed THP-1 monocytes was attenuated in the presence of selective inhibitors of ER IP_3R-associated Ca^{2+} channels (XestC) and MCU (Ru360), demonstrating that both ER and mitochondria are involved in NLRP3 inflammasome activation in human monocytes under stressful conditions. More specifically, our results showed that NLRP3 inflammasome activation in these conditions depends on mitochondrial Ca^{2+} uptake and also seems to be triggered by Ca^{2+} release from the ER through the IP_3R. This data, together with our findings showing enhanced ER-mitochondria contacts at MAMs and higher

mitochondrial Ca^{2+} uptake in TM-treated cells, suggest that ER-mitochondria communication plays a role in ER stress-induced activation of the NLRP3 inflammasome in THP-1 human monocytes. According to our results, NLRP3 inflammasome has been described as a general sensor for disturbances in cellular homeostasis, including for alterations in intracellular Ca^{2+} signaling [18]. Brough et al. implicated Ca^{2+} fluxes in NLRP3 inflammasome activation, demonstrating that IL-1β secretion depends on the release of Ca^{2+} from intracellular ER stores in ATP-treated murine macrophages [95]. More recently, Triantafilou and colleagues found that increased mitochondrial Ca^{2+} uptake and loss of mitochondrial membrane potential activate the NLRP3 inflammasome in human lung epithelial cells. These authors showed that secretion of IL-1β was reverted upon blockage of mitochondrial Ca^{2+} accumulation by MCU inhibition [96].

The above alterations induced by ER stress on THP-1 innate immune cells, namely, increased ER-mitochondria contact sites, changes in Ca^{2+} homeostasis, depolarization of mitochondria membrane, impaired mitochondrial dynamics and NLRP3 inflammasome activation, culminate in the compromise of cell viability. Accordingly, a close intersection between cell death and inflammasome activation has been described [97, 98]. Currently, pyroptosis is defined as the type of cell death dependent on inflammasome activation [99].

Sterile inflammation mediated by NLRP3 inflammasome activation is induced by multiple pathological conditions both in the peripheral immune system and in the CNS. Neuroinflammation has been strongly implicated in the pathophysiology of several CNS disorders, such as neurodegenerative and psychiatric diseases [100–102]. It is mainly caused by the activation of microglia, the primary resident innate immune cells in the CNS able to trigger an immunologic response [18]. Over the last few years, several stimuli have been described as activators of the NLRP3 inflammasome in microglia. For instance, it was shown that IL-1β secretion by microglia cells exposed to live *S. aureus* [103] or ceramide [104] is mediated by NLRP3 inflammasome activation. Furthermore, NLRP3 inflammasome has also been implicated in the innate immune response triggered by misfolded proteins such as the prion peptide PrP106-126 and alpha-synuclein [105–107]. Fibrillar Aβ and aggregated tau were also shown to induce the assembly and activation of NLRP3 inflammasome in mouse microglia [106, 108]. More recently, Molagoda and colleagues revealed that in BV2 microglial cells the canonical activation of NLRP3 inflammasome induced by LPS and ATP is regulated by ER stress, as supported by the increased expression of UPR markers [109]. Here, we presented a direct cause-effect relationship between ER stress and NLRP3 inflammasome activation in BV2 microglial cells, by showing that the induction of ER stress promotes the release of pro-inflammatory IL-1β, as well as the upregulation of pro-IL-1β and NLRP3.

Finally, NLRP3 inflammasome activation was further assessed in monocytes obtained from patients with a diagnosis of BD, a pathological condition associated with inflammation [110], as well as from matched healthy controls. It was found that BD innate immune cells are more susceptible to ER stress, as shown by increased NLRP3 protein levels, as well as higher levels of secreted IL-1β, upon TM exposure in BD patient-derived monocytes in comparison with control cells. Our results emphasize the role of NLRP3 inflammasome in pro-inflammatory status associated with BD, in accordance with previous studies [111, 112]. Kim and colleagues proposed the involvement of NLRP3 inflammasome in BD pathophysiology based on their findings obtained from the post-mortem analysis of frontal cortex from BD patients showing high levels of IL-1β and caspase-1, as well as upregulation of NLRP3 and ASC [112]. In fact, several studies have consistently reported elevated levels of pro-inflammatory cytokines in patients with BD [113]. For example, increased IL-1β levels were detected in the cerebrospinal fluid of euthymic BD patients and an altered brain cytokine profile was detected after manic/hypomanic episodes [114]. Recently, Magioncalda et al. correlated BD-associated immunological alterations with neuroanatomical changes, namely white matter microstructural abnormalities [115]. Furthermore, our results obtained from the analysis of the biochemical markers of inflammation in the blood samples derived from BD patients *vs* healthy controls, showing an increase in the levels of ferritin and leukocytes on subjects with BD diagnosis, and also a higher number of circulating monocytes, neutrophils and lymphocytes, further supported BD-associated inflammatory status these results agree with previous studies reporting that BD patients have altered numbers of these immune cells in peripheral blood [116, 117]. Moreover, clinical evidence of immune dysregulation in BD patients, including the development of autoimmune diseases such as rheumatoid arthritis and hyperthyroidism, as well as the high prevalence of chronic metabolic diseases such as diabetes and obesity, also reinforces the role of a sterile inflammatory phenotype in BD pathophysiology [110, 118, 119].

Conclusion

Several cellular events have been implicated in the initiation and/or progression of numerous human pathologies, such as compromised ER stress response, mitochondrial dysfunction, ER-mitochondria miscommunication, as well as innate immune disturbances, namely NLRP3 inflammasome activation. However, the mechanisms underlying activation of the NLRP3 inflammasome are still not fully understood.

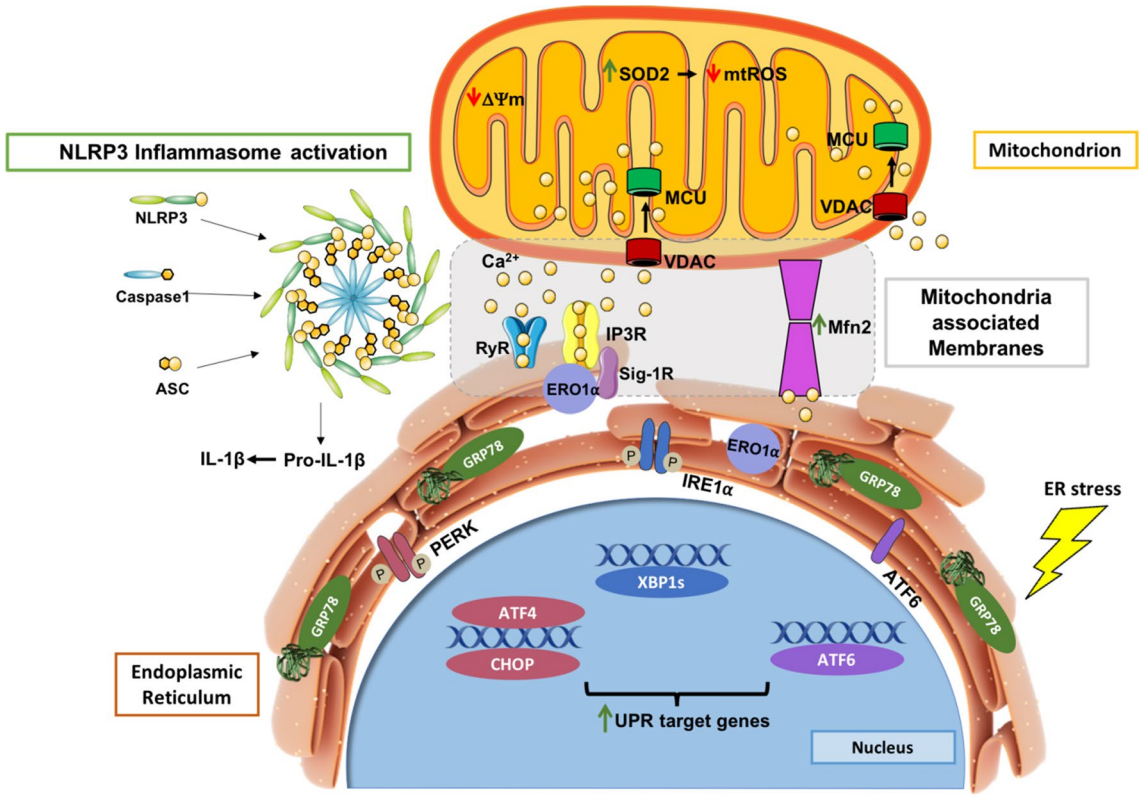

Fig. 12 ER-mitochondria communication is implicated in ER stress-induced NLRP3 inflammasome activation in the innate immune system. ER stress modulates the structure of mitochondria-associated membranes (MAMs) in human monocytes as demonstrated by the upregulation of chaperones that reside or that are translocated to these ER-mitochondria close contacts under severe/prolonged ER stress, and by the increment of the Mfn2 ER-mitochondria tethering protein. The proximity between both organelles occurs concomitantly with an early Ca^{2+} influx into mitochondria and depolarization of mitochondrial membrane, culminating in activation of the NLRP3 inflammasome and release of pro-inflammatory IL-1β that is also affected by the release of Ca^{2+} from the ER. Enhanced mitochondrial fusion to stimulate energy production can lead to the accumulation of dysfunctional mitochondrial compromising cell viability. Activation of antioxidant defenses within mitochondria to avoid ROS accumulation might represent a protective strategy that is not able to counteract chronic ER stress-induced sterile inflammation

Overall, the major findings achieved in this study using human THP-1 monocytes, a model of the peripheral innate immune system, demonstrate that ER stress affects the content of MAM-resident chaperones and increases the number of close ER-mitochondria contacts. It was also found that mitochondrial Ca^{2+} uptake under stress conditions is associated with enhanced fusion and inhibited fission, which might represent an attempt to preserve energy production. However, the accumulation of depolarized mitochondria, possibly due to impaired mitophagy, might compromise cell viability. Under these conditions, NLRP3 inflammasome was shown to be activated, leading to IL-1β release, by a ROS accumulation-independent mechanism, possibly due to stimulation of antioxidant defenses, namely SOD2. On the other hand, ER Ca^{2+} release, as well as mitochondrial Ca^{2+} uptake, were found to be implicated in ER stress-induced NLRP3 activation, further supporting the key role of ER-mitochondria communication in sterile inflammation induced by cellular stress. In summary, ER stress activates adaptive strategies in human monocytes to restore homeostasis. However, under chronic stress, pathological mechanisms are triggered and become prevalent leading to a pro-inflammatory status that culminates in loss of cell survival. Importantly, it was demonstrated that ER stress-induced NLRP3 inflammasome activation also occurs in CNS innate immune cells, namely in LPS-primed microglia. Finally, and as a proof of concept study, we disclosed that this mechanism occurs under pathological conditions as demonstrated by the exacerbated NLRP3 inflammasome activation in response to ER stress exhibited by monocytes obtained from BD patients, at early disease stages, in comparison with healthy controls, supporting that sterile inflammatory is implicated in BD pathophysiology.

In conclusion, this study contributes to elucidate the molecular mechanisms underlying NLRP3 inflammasome activation upon ER stress in the innate immune system, suggesting that ER-mitochondria communication plays a relevant role (Fig. 12). These findings might help to identify

novel therapeutic strategies and new diagnostic biomarkers for diseases associated with sterile inflammation, namely psychiatric illnesses such as BD.

Acknowledgements The authors thank Fernando Rodrigues, Director of the Department of Clinical Pathology from Hospital from the University of Coimbra (CHUC), for the biochemical analysis in peripheral blood isolated from BD patients and healthy controls.

Author contributions The presented experimental work carried out in THP-1 monocytes was performed by ACP with the collaboration of JDP, SC, IF and BN, BV2 microglial cells assays were conducted by RR. MAC contributed to monocyte's isolation from peripheral blood monuclear cells. MZ prepared samples and acquired the TEM images. NM, SM and AM selected BD patients and healthy controls to be included in the study. AC was responsible for collecting the hematological and biochemical parameters from BD patients and healthy controls. MTC and CFP designed the study, supervised the experiments and were also involved in the preparation of the manuscript. All authors read and approved the final manuscript.

Funding This work was funded by the European Regional Development Fund (ERDF), through the Centro 2020 Regional Operational Programme under project CENTRO-01-0145-FEDER-000012 (HealthyAging2020) and through the COMPETE 2020—Operational Programme for Competitiveness and Internationalisation and Portuguese national funds via FCT – Fundação para a Ciência e a Tecnologia, under projects POCI-01-0145-FEDER-028214 and POCI-01-0145-FEDER-029369 and UIDB/04539/2020 and UIDP/04539/2020. European Social Fund (Post-Doctoral Researcher Contract SFRH/BPD/101028/2014 to Rosa Resende). Ana Catarina Pereira is the recipient of PhD fellowship from FCT (SFRH/BD/148653/2019).

Availability of data and materials The datasets used and/or analyzed during the current study are available from the corresponding author on reasonable request.

Declarations

Conflict of interests The authors declare that they have no competing interests.

Ethics approval and consent to participate Human peripheral blood was collected by vein puncture from male BD patients and healthy gender- and age-matched controls, upon written informed consent and approval of the study by the Ethical Committee from Hospitals from University of Coimbra (CHUC), Portugal (150/CES, July 3rd).

Consent for publication Not applicable.

References

1. Filadi R, Theurey P, Pizzo P (2017) The endoplasmic reticulum-mitochondria coupling in health and disease: molecules, functions and significance. Cell Calcium 62:1–15. https://doi.org/10.1016/j.ceca.2017.01.003
2. Pfaffenseller B, Wollenhaupt-Aguiar B, Fries GR et al (2014) Impaired endoplasmic reticulum stress response in bipolar disorder: cellular evidence of illness progression. Int J Neuropsychopharmacol 17:1453–1463. https://doi.org/10.1017/S1461145714000443
3. Ron D, Walter P (2007) Signal integration in the endoplasmic reticulum unfolded protein response. Nat Rev Mol Cell Biol 8:519–529. https://doi.org/10.1038/nrm2199
4. Decuypere J-P, Monaco G, Bultynck G et al (2011) The IP3 receptor–mitochondria connection in apoptosis and autophagy. Biochim Biophys Acta Mol Cell Res 1813:1003–1013. https://doi.org/10.1016/J.BBAMCR.2010.11.023
5. Deegan S, Saveljeva S, Gorman AM, Samali A (2013) Stress-induced self-cannibalism: on the regulation of autophagy by endoplasmic reticulum stress. Cell Mol Life Sci 70:2425–2441. https://doi.org/10.1007/s00018-012-1173-4
6. Tsang KY, Chan D, Bateman JF, Cheah KSE (2010) In vivo cellular adaptation to ER stress: survival strategies with double-edged consequences. J Cell Sci 123:2145–2154. https://doi.org/10.1242/jcs.068833
7. Kim I, Xu W, Reed JC (2008) Cell death and endoplasmic reticulum stress: disease relevance and therapeutic opportunities. Nat Rev Drug Discov 7:1013–1030. https://doi.org/10.1038/nrd2755
8. Hetz C, Chevet E, Oakes SA (2015) Proteostasis control by the unfolded protein response. Nat Cell Biol 17:829–838. https://doi.org/10.1038/ncb3184
9. Spang A (2018) The endoplasmic reticulum-the caring mother of the cell. Curr Opin Cell Biol 53:92–96. https://doi.org/10.1016/j.ceb.2018.06.004
10. Li J, Zhang D, Brundel BJJM, Wiersma M (2019) Imbalance of ER and mitochondria interactions: prelude to cardiac ageing and disease? Cells 8:1617
11. Prinz WA (2014) Bridging the gap: membrane contact sites in signaling, metabolism, and organelle dynamics. J Cell Biol 205:759–769. https://doi.org/10.1083/jcb.201401126
12. Area-Gomez E, Del Carmen Lara CastilloTambini MMD et al (2012) Upregulated function of mitochondria-associated ER membranes in Alzheimer disease. EMBO J 31:4106–4123. https://doi.org/10.1038/emboj.2012.202
13. Missiroli S, Patergnani S, Caroccia N et al (2018) Mitochondria-associated membranes (MAMs) and inflammation. Cell Death Dis 9:329. https://doi.org/10.1038/s41419-017-0027-2
14. Rowland AA, Voeltz GK (2012) Endoplasmic reticulum–mitochondria contacts: function of the junction. Nat Rev Mol Cell Biol 13:607–625. https://doi.org/10.1038/nrm3440
15. van Vliet AR, Verfaillie T, Agostinis P (2014) New functions of mitochondria associated membranes in cellular signaling. Biochim Biophys Acta Mol Cell Res 1843:2253–2262. https://doi.org/10.1016/j.bbamcr.2014.03.009
16. Filadi R, Greotti E, Pizzo P (2018) Highlighting the endoplasmic reticulum-mitochondria connection: focus on mitofusin 2. Pharmacol Res 128:42–51
17. Guo H, Callaway JB, Ting JP-Y (2015) Inflammasomes: mechanism of action, role in disease, and therapeutics. Nat Med 21:677–687. https://doi.org/10.1038/nm.3893
18. Walsh JG, Muruve DA, Power C (2014) Inflammasomes in the CNS. Nat Rev Neurosci 15:84–97. https://doi.org/10.1038/nrn3638
19. Hanamsagar R, Hanke ML, Kielian T (2012) Toll-like receptor (TLR) and inflammasome actions in the central nervous system. Trends Immunol 33:333–342. https://doi.org/10.1016/j.it.2012.03.001
20. He Y, Hara H, Núñez G (2016) Mechanism and regulation of NLRP3 inflammasome activation. Trends Biochem Sci 41:1012–1021. https://doi.org/10.1016/j.tibs.2016.09.002
21. Gaidt MM, Ebert TS, Chauhan D et al (2016) Human monocytes engage an alternative inflammasome pathway. Immunity 44:833–846. https://doi.org/10.1016/j.immuni.2016.01.012

22. Bauernfeind FG, Horvath G, Stutz A et al (2009) Cutting edge: NF-kappaB activating pattern recognition and cytokine receptors license NLRP3 inflammasome activation by regulating NLRP3 expression. J Immunol 183:787–791. https://doi.org/10.4049/jimmunol.0901363
23. Franchi L, Eigenbrod T, Nunez G (2009) Cutting edge: TNF-alpha mediates sensitization to ATP and silica via the NLRP3 inflammasome in the absence of microbial stimulation. J Immunol 183:792–796. https://doi.org/10.4049/jimmunol.0900173
24. Malik A, Kanneganti T-D (2017) Inflammasome activation and assembly at a glance. J Cell Sci 130:3955–3963. https://doi.org/10.1242/jcs.207365
25. Kelley N, Jeltema D, Duan Y, He Y (2019) The NLRP3 inflammasome: an overview of mechanisms of activation and regulation. Int J Mol Sci. https://doi.org/10.3390/ijms20133328
26. Zhou R, Yazdi AS, Menu P, Tschopp J (2011) A role for mitochondria in NLRP3 inflammasome activation. Nature 469:221–225. https://doi.org/10.1038/nature09663
27. Subramanian N, Natarajan K, Clatworthy MR et al (2013) The adaptor MAVS promotes NLRP3 mitochondrial localization and inflammasome activation. Cell 153:348–361. https://doi.org/10.1016/j.cell.2013.02.054
28. Zhou Y, Tong Z, Jiang S et al (2020) The roles of endoplasmic reticulum in NLRP3 inflammasome activation. Cells 9:1219
29. de la Roche M, Hamilton C, Mortensen R et al (2018) Trafficking of cholesterol to the ER is required for NLRP3 inflammasome activation. J Cell Biol. https://doi.org/10.1083/JCB.201709057
30. Misawa T, Takahama M, Saitoh T (2017) Mitochondria–endoplasmic reticulum contact sites mediate innate immune responses. Adv Exp Med Biol 187–197
31. Resende R, Fernandes T, Pereira AC et al (2020) Mitochondria, endoplasmic reticulum and innate immune dysfunction in mood disorders: do mitochondria-associated membranes (MAMs) play a role? Biochim Biophys acta Mol basis Dis 1866:165752. https://doi.org/10.1016/j.bbadis.2020.165752
32. Pereira CF, Santos AE, Moreira PI et al (2019) Is Alzheimer's disease an inflammasomopathy? Ageing Res Rev. https://doi.org/10.1016/j.arr.2019.100966
33. McIntyre RS, Berk M, Brietzke E et al (2020) Bipolar disorders. Lancet 396:1841–1856
34. Berk M, Post R, Ratheesh A et al (2017) Staging in bipolar disorder: from theoretical framework to clinical utility. World Psychiatry 16:236–244. https://doi.org/10.1002/wps.20441
35. American Psychiatric Association (2013) Diagnostic and of statistical manual mental disorders. American Psychiatric Association, Washington, D.C.
36. Martins MJ, Palmeira L, Xavier A et al (2019) The clinical interview for psychotic disorders (CIPD): preliminary results on interrater agreement, reliability and qualitative feedback. Psychiatry Res 272:723–729. https://doi.org/10.1016/j.psychres.2018.12.176
37. Pereira AC, Madeira N, Morais S et al (2022) Mitochondria fusion upon SERCA inhibition prevents activation of the NLRP3 inflammasome in human monocytes. Cells 11:433. https://doi.org/10.3390/cells11030433
38. Nguyen L, Lucke-Wold BP, Mookerjee SA et al (2015) Role of sigma-1 receptors in neurodegenerative diseases. J Pharmacol Sci 127:17–29. https://doi.org/10.1016/j.jphs.2014.12.005
39. Simmen T, Herrera-Cruz MS (2018) Plastic mitochondria-endoplasmic reticulum (ER) contacts use chaperones and tethers to mould their structure and signaling. Curr Opin Cell Biol 53:61–69. https://doi.org/10.1016/j.ceb.2018.04.014
40. Li G, Mongillo M, Chin K-T et al (2009) Role of ERO1-α–mediated stimulation of inositol 1,4,5-triphosphate receptor activity in endoplasmic reticulum stress–induced apoptosis. J Cell Biol 186:783–792. https://doi.org/10.1083/jcb.200904060
41. Tesei A, Cortesi M, Zamagni A et al (2018) Sigma receptors as endoplasmic reticulum stress "gatekeepers" and their modulators as emerging new weapons in the fight against cancer. Front Pharmacol 9:711. https://doi.org/10.3389/fphar.2018.00711
42. Weng TY, Tsai SYA, Su TP (2017) Roles of sigma-1 receptors on mitochondrial functions relevant to neurodegenerative diseases. J Biomed Sci 24:1–14
43. Lehmann D, Tuppen HAL, Campbell GE et al (2019) Understanding mitochondrial DNA maintenance disorders at the single muscle fibre level. Nucleic Acids Res. https://doi.org/10.1093/nar/gkz472
44. Contino S, Porporato PE, Bird M et al (2017) Presenilin 2-dependent maintenance of mitochondrial oxidative capacity and morphology. Front Physiol. https://doi.org/10.3389/fphys.2017.00796
45. Li S, Bouzar C, Cottet-Rousselle C et al (2016) Resveratrol inhibits lipogenesis of 3T3-L1 and SGBS cells by inhibition of insulin signaling and mitochondrial mass increase. Biochim Biophys Acta Bioenerg. https://doi.org/10.1016/j.bbabio.2016.03.009
46. Kozhukhar N, Alexeyev MF (2019) Limited predictive value of TFAM in mitochondrial biogenesis. Mitochondrion. https://doi.org/10.1016/j.mito.2019.08.001
47. Srinivasan S, Guha M, Kashina A, Avadhani NG (2017) Mitochondrial dysfunction and mitochondrial dynamics—the cancer connection. Biochim Biophys Acta Bioenerg 1858:602–614. https://doi.org/10.1016/j.bbabio.2017.01.004
48. Moreira OC, Estébanez B, Martínez-Florez S et al (2017) Mitochondrial function and mitophagy in the elderly: effects of exercise. Oxid Med Cell Longev 2017:1–13. https://doi.org/10.1155/2017/2012798
49. Naon D, Zaninello M, Giacomello M et al (2016) Critical reappraisal confirms that mitofusin 2 is an endoplasmic reticulum–mitochondria tether. Proc Natl Acad Sci 113:11249–11254. https://doi.org/10.1073/pnas.1606786113
50. Ochoa CD, Wu RF, Terada LS (2018) ROS signaling and ER stress in cardiovascular disease. Mol Aspects Med 63:18–29. https://doi.org/10.1016/j.mam.2018.03.002
51. Vannuvel K, Renard P, Raes M, Arnould T (2013) Functional and morphological impact of ER stress on mitochondria. J Cell Physiol 228:1802–1818. https://doi.org/10.1002/jcp.24360
52. Chang WC, Di Capite J, Singaravelu K et al (2008) Local Ca2+ influx through Ca2+ release-activated Ca2+ (CRAC) channels stimulates production of an intracellular messenger and an intercellular pro-inflammatory signal. J Biol Chem. https://doi.org/10.1074/jbc.M705002200
53. Zha Q-B, Wei H-X, Li C-G et al (2016) ATP-induced inflammasome activation and pyroptosis is regulated by AMP-activated protein kinase in macrophages. Front Immunol 7:597. https://doi.org/10.3389/fimmu.2016.00597
54. Muneer A (2016) The neurobiology of bipolar disorder: an integrated approach. Chonnam Med J 52:18–37. https://doi.org/10.4068/cmj.2016.52.1.18
55. Pereira AC, Resende R, Morais S, et al (2017) The ups and downs of cellular stress: the "MAM hypothesis" for bipolar disorder pathophysiology. Int J Clin Neurosci Ment Heal 4:S04. https://doi.org/10.21035/ijcnmh.2017.4(Suppl.3).S04
56. Pereira AC, Oliveira J, Silva S et al (2021) Inflammation in Bipolar Disorder (BD): Identification of new therapeutic targets. Pharmacol Res 163:105325
57. Rajendran P, Chen Y-F, Chen Y-F et al (2018) The multifaceted link between inflammation and human diseases. J Cell Physiol 233:6458–6471. https://doi.org/10.1002/jcp.26479

58. So J-S (2018) Roles of endoplasmic reticulum stress in immune responses. Mol Cells 41:705–716. https://doi.org/10.14348/molcells.2018.0241
59. Menu P, Mayor A, Zhou R et al (2012) ER stress activates the NLRP3 inflammasome via an UPR-independent pathway. Cell Death Dis 3:e261. https://doi.org/10.1038/cddis.2011.132
60. Bravo R, Parra V, Gatica D et al (2013) Endoplasmic reticulum and the unfolded protein response. Int Rev Cell Mol Biol 301:215–290
61. Zhang B, Gao C, Li Y, Wang M (2018) D-chiro-inositol enriched *Fagopyrum tataricum* (L.) gaench extract alleviates mitochondrial malfunction and inhibits ER stress/JNK associated inflammation in the endothelium. J Ethnopharmacol 214:83–89. https://doi.org/10.1016/j.jep.2017.12.002
62. Li X, Zhu H, Huang H et al (2012) Study on the effect of IRE1α on cell growth and apoptosis via modulation PLK1 in ER stress response. Mol Cell Biochem 365:99–108. https://doi.org/10.1007/s11010-012-1248-4
63. Hwang J, Qi L (2018) Quality control in the endoplasmic reticulum: crosstalk between ERAD and UPR pathways. Trends Biochem Sci 43:593–605. https://doi.org/10.1016/J.TIBS.2018.06.005
64. Chen X, Zhong J, Dong D et al (2017) Endoplasmic reticulum stress-induced CHOP inhibits PGC-1α and causes mitochondrial dysfunction in diabetic embryopathy. Toxicol Sci 158:275–285. https://doi.org/10.1093/toxsci/kfx096
65. Tao YK, Shi J, Yu PL, Zhang GQ (2018) The role of endoplasmic reticulum stress-related apoptosis in vascular endothelium pathogenesis. Biomed Environ Sci 31:555–559. https://doi.org/10.3967/bes2018.076
66. Gilady SY, Bui M, Lynes EM et al (2010) Ero1α requires oxidizing and normoxic conditions to localize to the mitochondria-associated membrane (MAM). Cell Stress Chaperones 15:619–629. https://doi.org/10.1007/s12192-010-0174-1
67. Anelli T, Bergamelli L, Margittai E et al (2012) Ero1α regulates Ca^{2+} fluxes at the endoplasmic reticulum-mitochondria interface (MAM). Antioxid Redox Signal 16:1077–1087. https://doi.org/10.1089/ars.2011.4004
68. Seervi M, Sobhan PK, Joseph J et al (2013) ERO1α-dependent endoplasmic reticulum–mitochondrial calcium flux contributes to ER stress and mitochondrial permeabilization by procaspase-activating compound-1 (PAC-1). Cell Death Dis 4:e968–e968. https://doi.org/10.1038/cddis.2013.502
69. Hayashi T, Su T-P (2007) Sigma-1 receptor chaperones at the ER- mitochondrion interface regulate Ca2+ signaling and cell survival. Cell 131:596–610. https://doi.org/10.1016/j.cell.2007.08.036
70. Hashimoto K (2015) Activation of sigma-1 receptor chaperone in the treatment of neuropsychiatric diseases and its clinical implication. J Pharmacol Sci 127:6–9. https://doi.org/10.1016/j.jphs.2014.11.010
71. Bravo R, Vicencio JM, Parra V et al (2011) Increased ER-mitochondrial coupling promotes mitochondrial respiration and bioenergetics during early phases of ER stress. J Cell Sci 124:2143–2152. https://doi.org/10.1242/jcs.080762
72. Koshiba T, Detmer SA, Kaiser JT et al (2004) Structural basis of mitochondrial tethering by mitofusin complexes. Science 305(80):858–862. https://doi.org/10.1126/science.1099793
73. Ishihara N, Eura Y, Mihara K (2004) Mitofusin 1 and 2 play distinct roles in mitochondrial fusion reactions via GTPase activity. J Cell Sci. https://doi.org/10.1242/jcs.01565
74. Chen Y, Csordás G, Jowdy C et al (2012) Mitofusin 2-containing mitochondrial-reticular microdomains direct rapid cardiomyocyte bioenergetic responses via interorganelle Ca2+ crosstalk. Circ Res. https://doi.org/10.1161/CIRCRESAHA.112.266585
75. Schneeberger M, Dietrich MO, Sebastián D et al (2013) Mitofusin 2 in POMC neurons connects ER stress with leptin resistance and energy imbalance. Cell. https://doi.org/10.1016/j.cell.2013.09.003
76. Ainbinder A, Boncompagni S, Protasi F, Dirksen RT (2015) Role of Mitofusin-2 in mitochondrial localization and calcium uptake in skeletal muscle. Cell Calcium 57:14–24. https://doi.org/10.1016/j.ceca.2014.11.002
77. De Brito OM, Scorrano L (2008) Mitofusin 2 tethers endoplasmic reticulum to mitochondria. Nature. https://doi.org/10.1038/nature07534
78. Cosson P, Marchetti A, Ravazzola M, Orci L (2012) Mitofusin-2 independent juxtaposition of endoplasmic reticulum and mitochondria: an ultrastructural study. PLoS ONE. https://doi.org/10.1371/journal.pone.0046293
79. Filadi R, Greotti E, Turacchio G et al (2015) Mitofusin 2 ablation increases endoplasmic reticulum-mitochondria coupling. Proc Natl Acad Sci USA. https://doi.org/10.1073/pnas.1504880112
80. Santel A, Fuller MT (2001) Control of mitochondrial morphology by a human mitofusin. J Cell Sci 114:867–874
81. Zhu T, Chen JL, Wang Q et al (2018) Modulation of mitochondrial dynamics in neurodegenerative diseases: an insight into prion diseases. Front Aging Neurosci 10:366
82. Yoo S-M, Jung Y-K (2018) A molecular approach to mitophagy and mitochondrial dynamics. Mol Cells 41:18–26. https://doi.org/10.14348/molcells.2018.2277
83. Harris J, Deen N, Zamani S, Hasnat MA (2018) Mitophagy and the release of inflammatory cytokines. Mitochondrion 41:2–8. https://doi.org/10.1016/j.mito.2017.10.009
84. Knupp J, Arvan P, Chang A (2019) Increased mitochondrial respiration promotes survival from endoplasmic reticulum stress. Cell Death Differ. https://doi.org/10.1038/s41418-018-0133-4
85. Han J, Murthy R, Wood B et al (2013) ER stress signalling through eIF2α and CHOP, but not IRE1α, attenuates adipogenesis in mice. Diabetologia. https://doi.org/10.1007/s00125-012-2809-5
86. Santos CXC, Tanaka LY, Wosniak J, Laurindo FRM (2009) Mechanisms and implications of reactive oxygen species generation during the unfolded protein response: roles of endoplasmic reticulum oxidoreductases, mitochondrial electron transport, and NADPH oxidase. Antioxid Redox Signal 11:2409–2427
87. Bahar E, Kim H, Yoon H (2016) ER stress-mediated signaling: action potential and Ca2+ as key players. Int J Mol Sci 17:1558. https://doi.org/10.3390/ijms17091558
88. Carreras-Sureda A, Jaña F, Urra H et al (2019) Non-canonical function of IRE1α determines mitochondria-associated endoplasmic reticulum composition to control calcium transfer and bioenergetics. Nat Cell Biol. https://doi.org/10.1038/s41556-019-0329-y
89. Bagur R, Hajnóczky G (2017) Intracellular Ca2+ sensing: its role in calcium homeostasis and signaling. Mol Cell 66:780–788. https://doi.org/10.1016/j.molcel.2017.05.028
90. De La Fuente S, Lambert JP, Nichtova Z et al (2018) Spatial separation of mitochondrial calcium uptake and extrusion for energy-efficient mitochondrial calcium signaling in the heart. Cell Rep. https://doi.org/10.1016/j.celrep.2018.08.040
91. Wacquier B, Combettes L, Dupont G (2020) Dual dynamics of mitochondrial permeability transition pore opening. Sci Rep. https://doi.org/10.1038/s41598-020-60177-1
92. Fribley A, Zhang K, Kaufman RJ (2009) Regulation of apoptosis by the unfolded protein response. In: Erhardt P, Toth A (eds) Methods in molecular biology (Clifton, N.J.). Humana Press, Totowa, pp 191–204
93. Beretta M, Santos CX, Molenaar C, et al (2020) Nox4 regulates InsP 3 receptor-dependent Ca 2+ release into mitochondria to

promote cell survival. EMBO J. https://doi.org/10.15252/embj.2019103530
94. Hamilton C, Anand PK (2019) Right place, right time: localisation and assembly of the NLRP3 inflammasome. F1000Research 8:676. https://doi.org/10.12688/f1000research.18557.1
95. Brough D, Le Feuvre RA, Wheeler RD et al (2003) Ca $^{2+}$ stores and Ca $^{2+}$ entry differentially contribute to the release of IL-1β and IL-1α from murine macrophages. J Immunol 170:3029–3036. https://doi.org/10.4049/jimmunol.170.6.3029
96. Triantafilou K, Hughes TR, Triantafilou M, Morgan BP (2013) The complement membrane attack complex triggers intracellular Ca2+ fluxes leading to NLRP3 inflammasome activation. J Cell Sci 126:2903–2913. https://doi.org/10.1242/jcs.124388
97. Rashidi M, Wicks IP, Vince JE (2020) Inflammasomes and cell death: common pathways in microparticle diseases. Trends Mol Med 26:1003–1020
98. Tweedell RE, Malireddi RKS, Kanneganti TD (2020) A comprehensive guide to studying inflammasome activation and cell death. Nat Protoc. https://doi.org/10.1038/s41596-020-0374-9
99. Rühl S, Shkarina K, Demarco B et al (2018) ESCRT-dependent membrane repair negatively regulates pyroptosis downstream of GSDMD activation. Science 362(80):956–960. https://doi.org/10.1126/science.aar7607
100. Fourrier C, Singhal G, Baune BT (2019) Neuroinflammation and cognition across psychiatric conditions. CNS Spectr 24:4–15
101. Meyer JH, Cervenka S, Kim MJ et al (2020) Neuroinflammation in psychiatric disorders: PET imaging and promising new targets. The Lancet Psychiatry 7:1064–1074
102. Narayanaswami V, Dahl K, Bernard-Gauthier V et al (2018) Emerging PET radiotracers and targets for imaging of neuroinflammation in neurodegenerative diseases: Outlook beyond TSPO. Mol Imaging 17:1–25
103. Hanamsagar R, Torres V, Kielian T (2011) Inflammasome activation and IL-1β/IL-18 processing are influenced by distinct pathways in microglia. J Neurochem 119:736–748. https://doi.org/10.1111/j.1471-4159.2011.07481.x
104. Scheiblich H, Schlütter A, Golenbock DT et al (2017) Activation of the NLRP3 inflammasome in microglia: the role of ceramide. J Neurochem 143:534–550. https://doi.org/10.1111/jnc.14225
105. Codolo G, Plotegher N, Pozzobon T et al (2013) Triggering of inflammasome by aggregated α-synuclein, an inflammatory response in synucleinopathies. PLoS ONE 8:e55375. https://doi.org/10.1371/journal.pone.0055375
106. Halle A, Hornung V, Petzold GC et al (2008) The NALP3 inflammasome is involved in the innate immune response to amyloid-β. Nat Immunol 9:857–865. https://doi.org/10.1038/ni.1636
107. Shi F, Yang L, Kouadir M et al (2012) The NALP3 inflammasome is involved in neurotoxic prion peptide-induced microglial activation. J Neuroinflammation 9:570. https://doi.org/10.1186/1742-2094-9-73
108. Stancu I-C, Cremers N, Vanrusselt H et al (2019) Aggregated Tau activates NLRP3–ASC inflammasome exacerbating exogenously seeded and non-exogenously seeded Tau pathology in vivo. Acta Neuropathol 137:599–617. https://doi.org/10.1007/s00401-018-01957-y
109. Molagoda IMN, Lee KT, Choi YH, Kim GY (2020) Anthocyanins from *Hibiscus syriacus* L. Inhibit oxidative stress-mediated apoptosis by activating the Nrf2/HO-1 signaling pathway. Antioxidants. https://doi.org/10.3390/antiox9010042
110. Fries GR, Walss-Bass C, Bauer ME, Teixeira AL (2019) Revisiting inflammation in bipolar disorder. Pharmacol Biochem Behav 177:12–19
111. Scaini G, Barichello T, Fries GR et al (2019) TSPO upregulation in bipolar disorder and concomitant downregulation of mitophagic proteins and NLRP3 inflammasome activation. Neuropsychopharmacology. https://doi.org/10.1038/s41386-018-0293-4
112. Kim HK, Andreazza AC, Elmi N et al (2016) Nod-like receptor pyrin containing 3 (NLRP3) in the post-mortem frontal cortex from patients with bipolar disorder: a potential mediator between mitochondria and immune-activation. J Psychiatr Res 72:43–50. https://doi.org/10.1016/j.jpsychires.2015.10.015
113. Sayana P, Colpo GD, Simões LR et al (2017) A systemic review of evidence for the role of inflammatory biomarkers in bipolar patients. J Psychiatr Res 92:160–182
114. Söderlund J, Olsson S, Samuelsson M et al (2011) Elevation of cerebrospinal fluid interleukin-1β in bipolar disorder. J Psychiatry Neurosci 36:114–118. https://doi.org/10.1503/jpn.100080
115. Magioncalda P, Martino M, Tardito S et al (2018) White matter microstructure alterations correlate with terminally differentiated CD8+ effector T cell depletion in the peripheral blood in mania: combined DTI and immunological investigation in the different phases of bipolar disorder. Brain Behav Immun. https://doi.org/10.1016/j.bbi.2018.04.017
116. Munkholm K, Jacoby AS, Lenskjold T et al (2018) Leukocytes in peripheral blood in patients with bipolar disorder—trait and state alterations and association with levels of cytokines and C-reactive protein. Psychiatry Res. https://doi.org/10.1016/j.psychres.2018.01.022
117. Barbosa IG, Rocha NP, Assis F et al (2015) Monocyte and lymphocyte activation in bipolar disorder: a new piece in the puzzle of immune dysfunction in mood disorders. Int J Neuropsychopharmacol. https://doi.org/10.1093/ijnp/pyu021
118. Kupfer DJ (2005) The increasing medical burden in bipolar disorder. JAMA 293:2528. https://doi.org/10.1001/jama.293.20.2528
119. SayuriYamagata A, Brietzke E, Rosenblat JD et al (2017) Medical comorbidity in bipolar disorder: the link with metabolic-inflammatory systems. J Affect Disord 211:99–106. https://doi.org/10.1016/j.jad.2016.12.059